

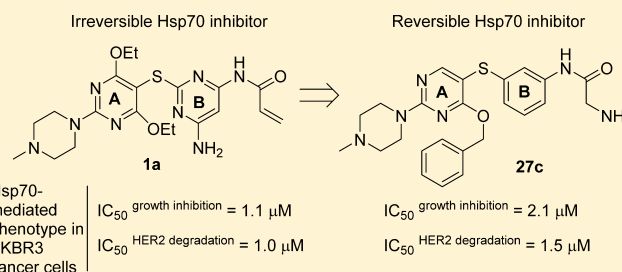
Heat Shock Protein 70 Inhibitors. 2. 2,5'-Thiodiprimidines, 5-(Phenylthio)pyrimidines, 2-(Pyridin-3-ylthio)pyrimidines, and 3-(Phenylthio)pyridines as Reversible Binders to an Allosteric Site on Heat Shock Protein 70

Tony Taldone,^{*,†} Yanlong Kang,^{†,§} Hardik J. Patel,[†] Maulik R. Patel,[†] Pallav D. Patel,[†] Anna Rodina,[†] Yogita Patel,[‡] Alexander Gozman,^{†,||} Ronnie Maharaj,[†] Cristina C. Clement,^{†,⊥} Alvin Lu,[†] Jason C. Young,[‡] and Gabriela Chiosis^{*,†}

[†]Program in Molecular Pharmacology and Chemistry and Department of Medicine, Memorial Sloan-Kettering Cancer Center, New York, New York 10021, United States

[‡]Groupe de Recherche Axé sur la Structure des Protéines, Department of Biochemistry, McGill University, Montreal, Quebec, Canada H3G 0B1

ABSTRACT: The discovery and development of heat shock protein 70 (Hsp70) inhibitors is currently a hot topic in cancer. In the preceding paper in this issue (10.1021/jm401551n), we have described structure–activity relationship studies in the first Hsp70 inhibitor class rationally designed to bind to a novel allosteric pocket located in the N-terminal domain of the protein. These ligands contained an acrylamide to take advantage of an active cysteine embedded in the allosteric pocket and acted as covalent protein modifiers upon binding. Here, we perform chemical modifications around the irreversible inhibitor scaffold to demonstrate that covalent modification is not a requirement for activity within this class of compounds. The study identifies derivative **27c**, which mimics the biological effects of the irreversible inhibitors at comparable concentrations. Collectively, the back-to-back manuscripts describe the first pharmacophores that favorably and selectively interact with a never explored pocket in Hsp70 and provide a novel blueprint for a cancer-oriented development of Hsp70-directed ligands.



■ INTRODUCTION

The heat shock protein 70 (Hsp70) is a molecular chaperone which plays an important function in protein homeostasis as well as in cell signaling and survival.^{1,2} Some of its functions include folding newly synthesized peptides, refolding misfolded proteins, assembling multiprotein complexes, and transporting proteins across cellular membranes. In addition to these housekeeping functions, Hsp70 is an important regulator of malignant transformation, both through its role as a powerful antiapoptotic protein and as a cochaperone of heat shock protein 90 (Hsp90).^{3–5} As a cochaperone of Hsp90, Hsp70 is thought to load client proteins onto the Hsp90 machinery through the action of another cochaperone, heat shock organizing protein (HOP).^{6,7} The Hsp90 machinery is an important mechanism by which cancer cells regulate the function of several cancer-driving proteins, such as those involved in altered signaling, the cell cycle, and transcriptional regulation. Indeed, it is primarily for this reason that Hsp90 has been actively pursued as an anticancer target.^{8,9} As an antiapoptotic molecule, Hsp70 acts at multiple points in the apoptotic pathway to prevent cell death.^{3–5} Due to these functions, it is not surprising that Hsp70 is frequently

overexpressed in cancer, where the elevated expression is furthermore believed to be a cause of or to lead to resistance to chemotherapy and other treatments.¹⁰ These dual roles of Hsp70 in cancer, i.e., cochaperone of Hsp90 and antiapoptotic molecule, suggest that inhibition of Hsp70 may offer a valuable anticancer strategy, as supported by Hsp70 knockdown studies.¹¹ Indeed, Hsp70 is an important and highly sought after cancer target,^{5,12,13} and as such it is of no surprise that the discovery and development of Hsp70 inhibitors is currently a hot topic.^{3–5}

To identify druglike Hsp70 inhibitors, we took a structure-based approach. In the first preceding paper in this issue, we described the development of inhibitors that target an allosteric pocket of Hsp70 located in the N-terminal domain of the protein.¹⁴ This pocket, not evident in the available crystal structures of Hsp70, has been recently identified by us through computational analyses.¹⁵ Thus, in the absence of an appropriate X-ray structure of human Hsp70, we used this homology model to design ligands that could bind to the

Received: October 4, 2013

Published: February 18, 2014

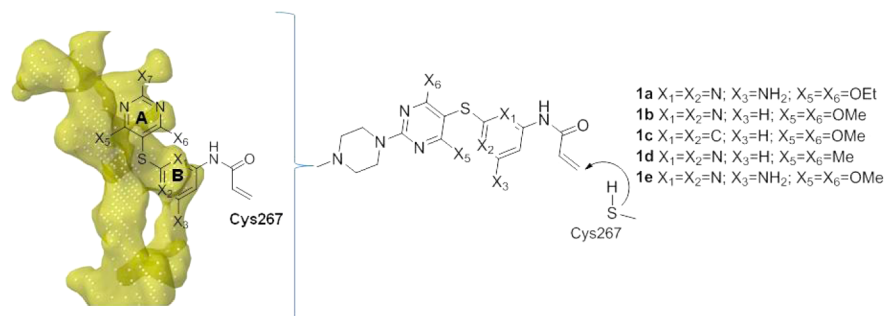


Figure 1. Chemical structure of acrylamide-containing 2,5'-thiodipyrimidine and 5-(phenylthio)pyrimidine scaffold Hsp70 inhibitors that were designed to insert into the Hsp70 allosteric pocket and form a covalent bond with Cys267 upon binding. The yellow surface shows the geometry of the allosteric pocket as determined by SiteMap (Schrodinger LLC, New York).

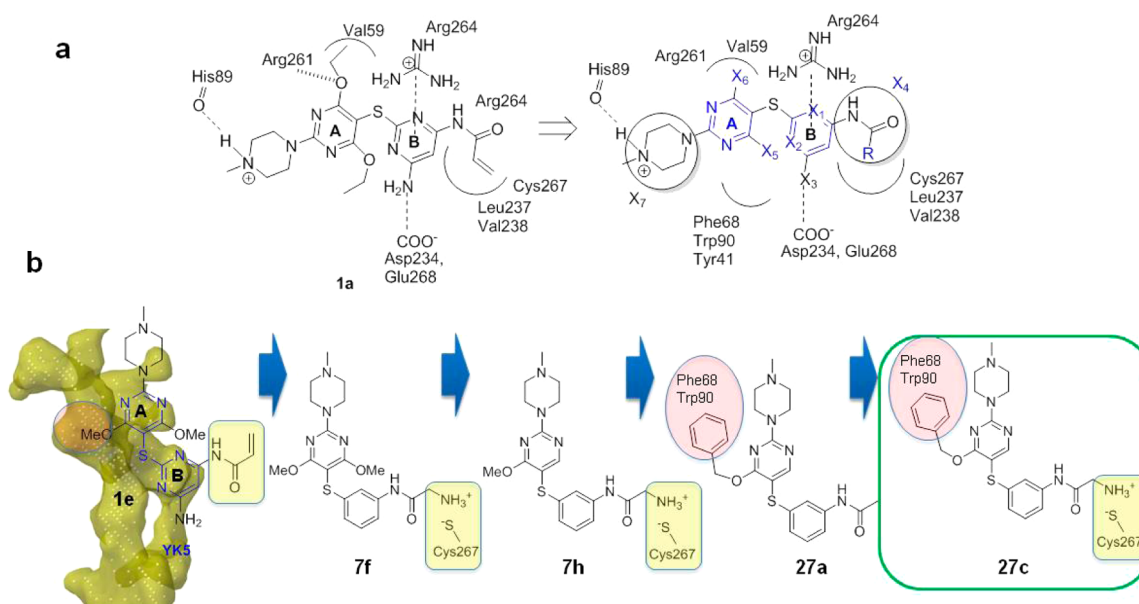


Figure 2. Design of the reversible Hsp70 inhibitors and their proposed mode of interaction with the Hsp70 pocket. (a) General strategy that indicates modifications that are explored here in the design of reversible inhibitors (highlighted in blue). (b) Step-by-step process that highlights key modifications that led to **27c**, a reversible Hsp70 binder of activity rivaling that of the most potent irreversible inhibitor **1e**.

Hsp70 allosteric pocket. Because the pocket also harbors a potentially reactive cysteine residue, the initially designed inhibitors, all built around the 2,5'-thiodipyrimidine and 5-(phenylthio)pyrimidine scaffolds, also incorporated an acrylamide moiety suitably positioned to interact with this amino acid upon insertion into the binding site (Figure 1). This body of work led to the identification of low micromolar inhibitors of Hsp70 with a good cell permeability profile and potent and selective biological activity in several cancer cells through an Hsp70-mediated mechanism of action. Our data indicated a good fit for these molecules inside the Hsp70 pocket, suggesting that enthalpy played an important role in their interaction with the protein.^{14,15}

In addition to being good leads, these compounds were also useful in demonstrating the therapeutic relevance of inhibiting the novel allosteric Hsp70 pocket as a potential anticancer approach.¹⁵ Specifically, by inserting into the allosteric pocket, these inhibitors alter the oncogenic Hsp70–Hsp90–client complexes, resulting in degradation of Hsp90–Hsp70–onco-client proteins and inhibition of cell growth and induction of apoptosis. They do so without activating a feedback heat shock response,¹⁵ a mechanism believed to be responsible for limiting the anticancer activity of Hsp90 inhibitors.¹⁶ The Hsp90–

Hsp70 machinery is also a known repressor of heat shock factor 1 (HSF-1).¹⁶ Inhibition of Hsp90, but not depletion of the Hsp90 cochaperones Hsp70, HOP, HIP, p23, and CyP40, led to HSF-1 activation, possibly because while these cochaperones participate with Hsp90 in the regulation of HSF-1, only Hsp90 plays a nonredundant role in repressing its heat shock activation ability.¹⁶ Activation of HSF-1 has a protective effect on the cancer cell as it leads to the upregulation of antiapoptotic molecules.⁵ Thus, Hsp70 allosteric inhibitors by differentiating between the regulatory activity of the Hsp90–Hsp70 machinery on onco-clients and on HSF-1 may result in more robust apoptosis in cancer cells when compared to Hsp90 inhibitors.

Here we focus on the identification of inhibitors that act on Hsp70 through reversible binding into the allosteric pocket. Although covalent inhibition may offer certain advantages (i.e., maintaining activity against mutations and the ability to inhibit the target in the presence of millimolar concentrations of ATP within the cell) and can be desirable in some instances, it may come with some drawbacks.¹⁷ Because of the presence of a reactive moiety, covalent inhibitors have a greater potential for off-target effects, such as inherent reactivity toward nonspecific thiols such as glutathione.¹⁸ Therefore, we desired molecules

that could also act in this pocket in a reversible manner. At this early point in Hsp70 drug discovery, it is not clear which mode is best; therefore, we thought it wise to pursue both, and in this paper we show our initial efforts in the elaboration of a covalent inhibitor targeting the allosteric site into a reversible non-competitive inhibitor of low micromolar potency.

DESIGN OF REVERSIBLE LIGANDS OF THE HSP70 ALLOSTERIC BINDING SITE

The design of reversible ligands for the allosteric Hsp70 pocket took advantage of our knowledge on the geometry of the allosteric pocket¹⁵ and the structure–activity relationship (SAR) we have learned from previous studies in the irreversible ligand series¹⁴ (Figure 2). Our tactic was to first take a localized approach in an attempt to phase out the covalent binding potential and to maximize noncovalent binding in this immediate region (modification on X₄). Then we took a global molecular perspective to probe and to enhance interaction in other parts of the molecule (modification on X₃, rings A and B, X₅, and X₆). Specifically, our modifications focused on replacing the acrylamide (X₄) with a favorable noncovalent modifying functionality and on altering the nature of rings A and B (Figure 2a, highlighted in blue). They then aimed to gain additional favorable enthalpy by filling out a hydrophobic pocket now only occupied by small X_{5,6} groups such as methoxy (Figure 2a, highlighted in blue, and Figure 2b, red circle). Favorable modifications, such as methylpiperazine at position X₇, were left mostly unchanged (Figure 2a).

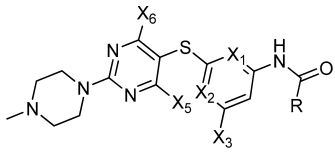
Thus, our overall design strategy entailed (1) determination of the extent of dependence of covalent modification for activity by replacing the acrylamide with groups that could provide favorable but noncovalent interaction with cysteine, (2) exploration of the SAR to maximize noncovalent interactions within the pocket occupied by acrylamide, and (3) exploration of the SAR in other parts of the molecule to maximize binding affinity.

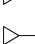
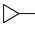
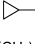
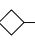
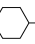
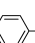
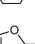
MAJOR MODIFICATIONS

Modification X₄. Modifying the acrylamide was based on several observations. As mentioned above, our modeling studies indicated that the region of Hsp70 occupied by X₄ also contained Leu237, Val238, Arg264, Asp234, and Lys271 in addition to the reactive Cys267 (Figure 2a). While the ability to form a covalent bond with the cysteine added significantly to the potency of the irreversible inhibitors, modeling studies indicated that the alkene moiety of the acrylamide group was positioned to also form hydrophobic interactions with adjacent protein residues, including Leu237 and Val238, while its carbonyl was poised to form electrostatic interactions with Arg264 (Figure 2a). Therefore, we reasoned that suitable groups substituted at X₄ would be capable of interacting with these residues in a wholly noncovalent manner. In our initial design of reversible ligands, we kept the amide functionality of X₄ but modified the alkene with a variety of groups (R, Figure 2a) incapable of interacting with cysteine covalently. These included alkyl groups of various sizes as well as aryl groups (R = methyl, ethyl, cyclopropyl, cyclobutyl, cyclohexyl, *n*-heptyl, allyl, phenyl, and furanyl) to probe the extent of modifications allowed by the pocket at this position. We also replaced the acrylamide with substituents that could potentially establish an ionic pair interaction with the S⁻ of Cys267 (i.e., ionizable

amines such as in **7f** (R = aminomethyl) and **9** (R = 2-(dimethylamino)ethyl)) (Tables 1 and 2).

Table 1

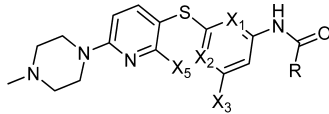


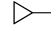
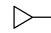
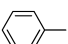
Compd.	X ₁ =X ₂	X ₃	X ₅	X ₆	R	IC ₅₀ (μM)	IC ₅₀ (μM)
						growth inhibition ^a	caspace-activation ^b
1a	N	-NH ₂	-OC ₂ H ₅	-OC ₂ H ₅	CH ₂ =CH-	0.89±0.2	4±0
3a	N	-NH ₂	-OC ₂ H ₅	-OC ₂ H ₅	CH ₃ CH ₂ -	51.4±5.0	37±3
1b	N	-H	-OCH ₃	-OCH ₃	CH ₂ =CH-	1.25±0.7	4±0
4b	N	-H	-OCH ₃	-OCH ₃	CH ₃ CH ₂ -	NA	142±17
1c	C	-H	-OCH ₃	-OCH ₃	CH ₂ =CH-	7.8±1.1	NA
7a	C	-H	-OCH ₃	-OCH ₃	CH ₃ CH ₂ -	NA	65±5
1d	N	-H	-CH ₃	-CH ₃	CH ₂ =CH-	NA	6±2
4c	N	-H	-CH ₃	-CH ₃	CH ₃ CH ₂ -	NA	98±27
3c	N	-NH ₂	-OCH ₃	-OCH ₃	CH ₃ -	NA	165±30
4a	N	-H	-OCH ₃	-OCH ₃	CH ₃ -	NA	150±10
3b	N	-NH ₂	-OC ₂ H ₅	-OC ₂ H ₅		NA	95±30
7b	N	-H	-OCH ₃	-OCH ₃		NA	24±1
4e	N	-H	-CH ₃	-CH ₃		60.5±4.2	68±21
3d	N	-NH ₂	-OCH ₃	-OCH ₃	CH ₃ (CH ₂) ₅ CH ₂ -	NA	>50
7c	C	-H	-OCH ₃	-OCH ₃		47.2±1.2	60±2
7d	C	-H	-OCH ₃	-OCH ₃		NA ^c	NA ^c
7e	C	-H	-OCH ₃	-OCH ₃		8.1±0.8	8±1
4d	N	-H	-CH ₃	-CH ₃		30.3±3.0	32±2
7g	C	-H	-OCH ₃	-OCH ₃	CH ₂ =CHCH ₂ -	NA	65±5
7f	C	-H	-OCH ₃	-OCH ₃	NH ₂ CH ₂ -	22.5±6.0	18±3
9	N	-NH ₂	-OCH ₃	-OCH ₃	(CH ₃) ₂ NCH ₂ CH ₂ -	14.7±3.3	25±10
7h	C	-H	-OCH ₃	-H	NH ₂ CH ₂ -	25.2±1.3	13±1

^aInhibition of growth measured in Kasumi-1 acute myeloid leukemia cells. Values are the mean ± SEM. ^bCaspase-3,7 activation measured in MOLM13 acute myeloid leukemia cells. Values are the mean ± SEM. ^cInsoluble.

Ring B. Ring B is predicted to occupy the lower part of the binding site that also contains Arg264. Thus, the ligand's interaction with the pocket could potentially be stabilized by cation– π interactions between the aromatic ring of ring B and the guanidine group of arginine (Figure 2a).¹⁹ Cation– π interactions play an important role in protein structure^{20,21} and molecular recognition^{19,22,23} and can contribute significantly to the binding energy of a ligand.²⁴ Such interactions are more likely to occur between an electron-rich π system (i.e., phenyl, ethylene, acetylene) and a neighboring cation and furthermore are generally favored with heterocycles that incorporate lone pair electrons into the aromatic system (i.e., indole, pyrrole) and become deactivated when the lone pair does not contribute to aromaticity (i.e., pyridine, pyrimidine).²⁵ In the irreversible series, pyrimidine was favored for ring B; the two nitrogen

Table 2



Compd.	X ₁ =X ₂	X ₃	X ₅	R	IC ₅₀ (μM)	
					growth inhibition ^a	IC ₅₀ (μM) caspase-activation ^b
14a	N	-H	-OCH ₃	CH ₃ CH ₂ -	NA	102±3
16a	C	-NH ₂	-OCH ₃	CH ₃ CH ₂ -	NA	39±5
14b	N	-NH ₂	-OCH ₃		58.5	63±2
16b	C	-NH ₂	-OCH ₃		36.4	32±8
16c	C	-H	-OCH ₃		4.7	20±1
16d	C	-H	-OCH ₃	NH ₂ CH ₂ -	19.1	21±6
21	C	-H	-OH	NH ₂ CH ₂ -	NA	>250

^aInhibition of growth measured in Kasumi-1 acute myeloid leukemia cells. ^bCaspase-3,7 activation measured in MOLM13 acute myeloid leukemia cells. Values are the mean ± SEM.

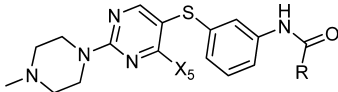
atoms of the pyrimidine ring rendered the ring more electron deficient, thus activating the acrylamide's Michael acceptor capability.¹⁴ In the reversible series, on the other hand, electron-rich B rings should be favored over electron-deficient ones because of their higher propensity toward cation- π interactions with Arg264 (Figure 2a). To test the hypothesis, we made compounds in which ring B was either phenyl (i.e., activating) or pyrimidine (i.e., deactivating) (Tables 1 and 2).

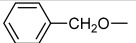
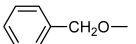
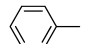
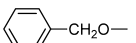
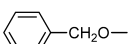
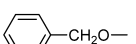
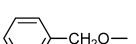
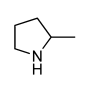
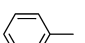
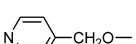
Ring A and Substituents X_{5,6}. Ring A and its substituents X₅ and X₆ are placed midpocket. Our initial investigations have mainly explored small substituents at this position such as methoxy, ethoxy, and methyl.¹⁴ This site, however, provides opportunity for substantial gains in binding affinity. It is lined by amino acids that could provide hydrophobic (Val59, Tyr41, Phe68, Trp90) and electrostatic (Arg261) interactions with the ligand (Figure 2a). Therefore, we explored here the effects of larger substituents on ring A, especially those poised for interactions within the lipophilic pocket formed by Tyr41, Phe68, and Trp90, such as derivatives in which X₅ contains an aryl (red circle in Figure 2b and Table 3). We also disrupted the symmetry of these molecules around ring A by probing monosubstitution of the ring (X₅ ≠ X₆ = H, Figure 2b). The representative SAR in this series is presented in Table 3.

MINOR MODIFICATIONS

Modification X₃. Ring B orients its X₃ substituent toward several important pocket residues such as Asp234 and Glu268 (X₃ is NH₂ in 1a, Figure 2a). NH₂ at this position is poised to form hydrogen bonds with their carboxylate groups, and we retained this functionality from the irreversible series in the design of new derivatives. The introduction of an -NH₂ at this position was synthetically challenging when ring B was phenyl, and for these, hydrogen was introduced at X₃. Thus, all compounds of this series contain either an NH₂ or a H at position X₃.

Table 3



Compd.	X ₅	R	IC ₅₀ (μM)	
			growth inhibition ^a	IC ₅₀ (μM) caspase-activation ^b
27a		CH ₃ -	5.2	10.2±3.2
27b			3.1	4.1±1.0
27c		NH ₂ CH ₂ -	2.3	1.9±0.2
27d		NH ₂ (CH ₃)CH-	4.8	2.0±0.1
27e		NH ₂ [(CH ₃) ₂ CH]CH-	3.1	2.4±0.3
27f			2.9	1.7±0.1
27g		NH ₂ CH ₂ -	20.8	25.2±2.2
27h		NH ₂ CH ₂ -	10.7	7.8±0.8

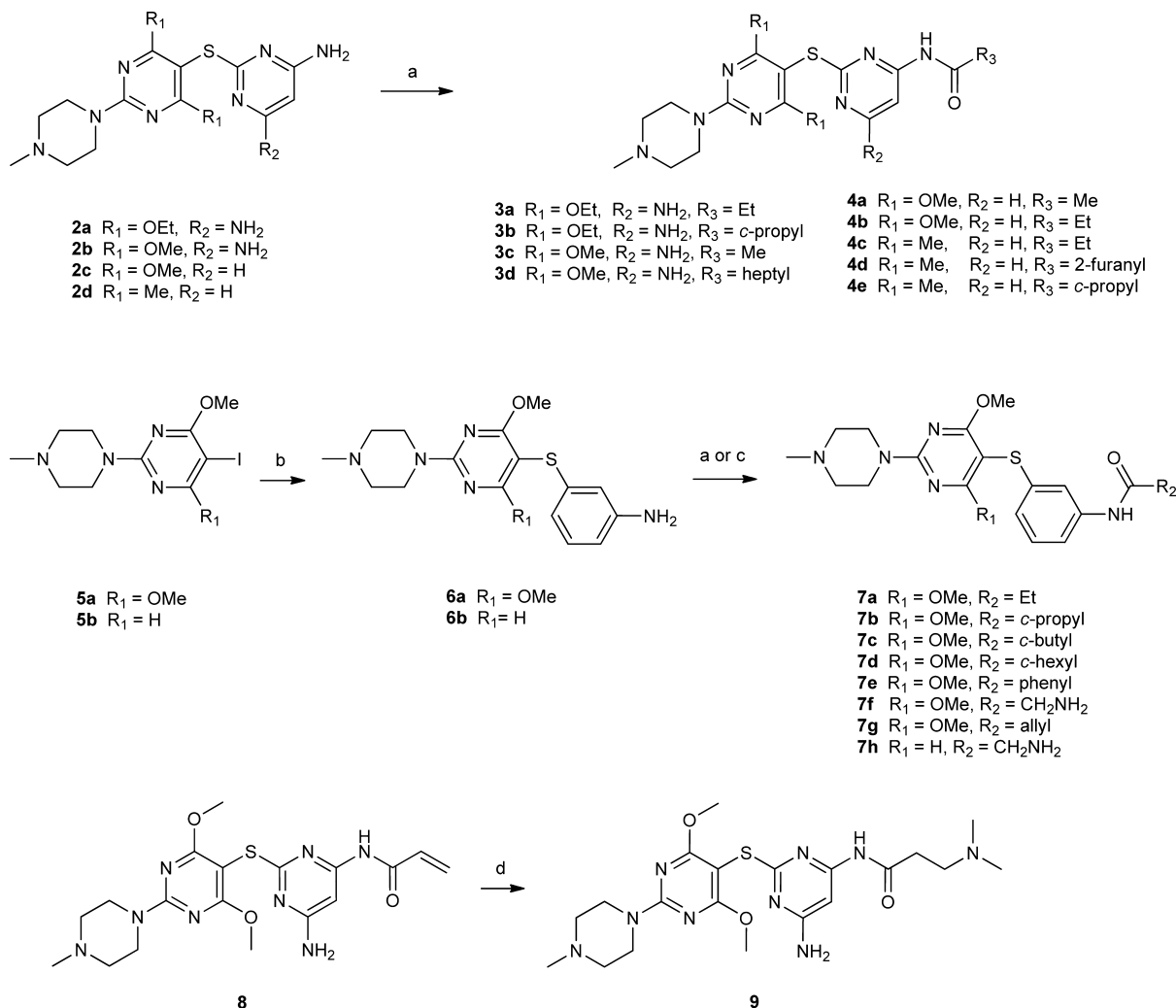
^aInhibition of growth measured in Kasumi-1 acute myeloid leukemia cells. ^bCaspase-3,7 activation measured in MOLM13 acute myeloid leukemia cells. Values are the mean ± SEM.

Modification X₇. Our previous SAR also showed that *N*-methylpiperazine was a preferred substituent on ring A at position X₇, presumably because of a proper fit in the minor groove located at the exit of the binding site and because it could form a hydrogen bond interaction with the backbone carbonyl of His89 (Figure 2a for 1a). As a result, X₇ was unchanged in the design of the novel derivatives described here.

CHEMISTRY

The synthesis of all designed compounds evaluated in this study is shown in Schemes 1–3. Target compounds 3a–d and 4a–e were prepared by reaction of 2a–d with the appropriate acid chloride (Scheme 1). Similarly, target compounds 7a–h were prepared by reaction of 6a,b with the appropriate acid chloride (Scheme 1). Thioethers 6a and 6b were prepared by CuI/neocuproine-catalyzed coupling of iodo derivative 5a or 5b, respectively, with 3-aminothiophenol (Scheme 1). 9 was prepared by Michael addition of dimethylamine to 8 with DBU (Scheme 1).

The synthesis of pyridine derivatives is shown in Scheme 2. Bromopyridine 10 was reacted with *N*-methylpiperazine at 130 °C for 16 h to give 11 in 88% yield. 12 was obtained in 95% yield following reaction of 11 with NIS at rt. 12 was coupled to 4-amino-2-mercaptopyrimidine with CuI/neocuproine to give thioether 13 in 60% yield. Acylation of 13 with propionyl chloride or cyclopropanecarbonyl chloride resulted in 14a or 14b, respectively. Coupling of 12 with 3-aminothiophenol resulted in 15, which was acylated with various acid chlorides to

Scheme 1^a

^aReagents and conditions: (a) acid chloride, Et₃N, dioxane or CH₂Cl₂, rt; (b) 3-aminothiophenol, neocuproine, CuI, K₂CO₃, DMF, 120 °C; (c) Boc-glycine, EDCI, DMAP, Et₃N, CH₂Cl₂, rt, then TFA, rt; (d) dimethylamine, DBU, CH₃CN, rt.

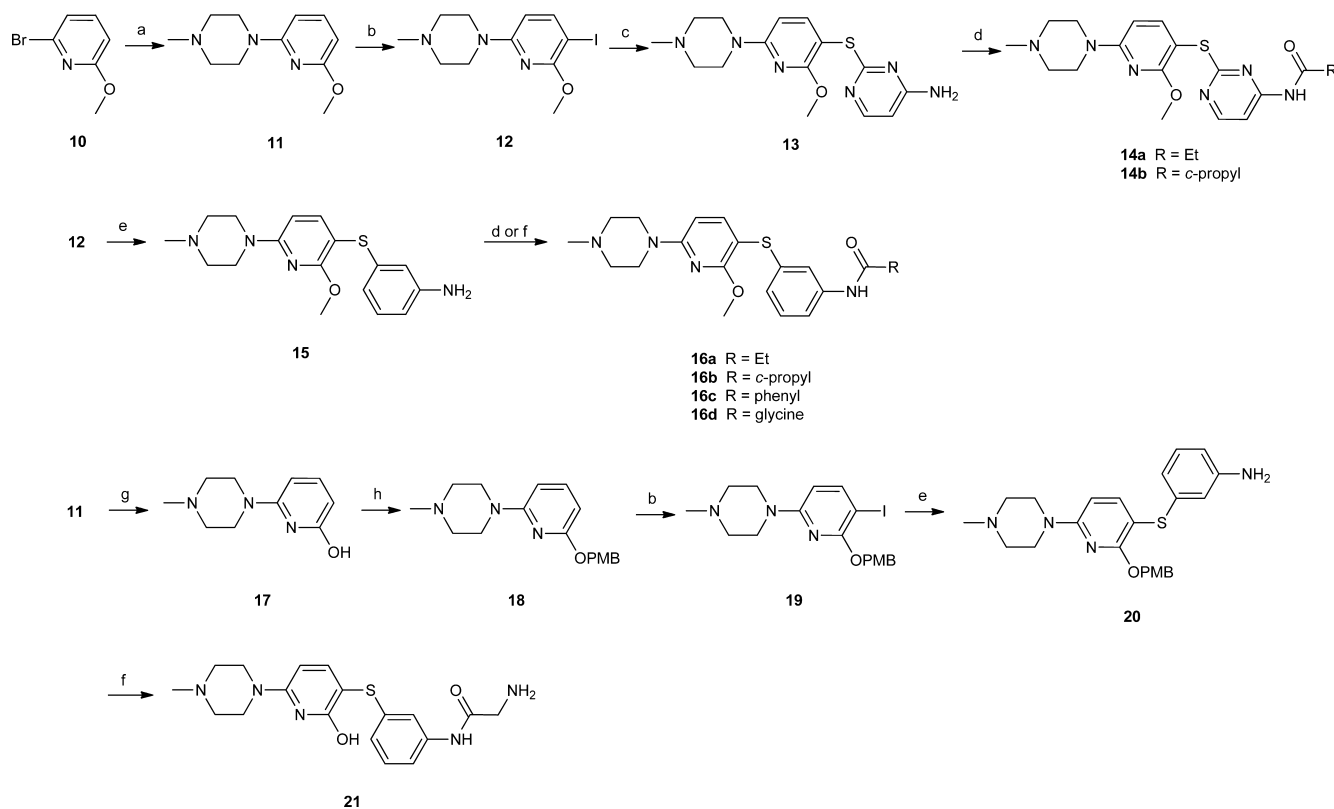
give target compounds **16a–d**. **17** was obtained from demethylation of **11** by refluxing in 48% HBr(aq) along with a catalytic amount of tetrabutylammonium bromide. Following PMB protection and reaction with NIS, iodo derivative **19** was obtained, which was coupled with 3-aminothiophenol to give thioether **20**. Reaction of **20** with Boc-glycine and subsequent deprotection with TFA resulted in **21**.

Target compounds **27a–f** were synthesized as shown in Scheme 3. First, 2,4-dichloropyrimidine (**22**) was reacted with benzyl alcohol under PTC conditions to result in a regioisomeric mixture of the desired 4-(benzyloxy)-2-chloropyrimidine (**23a**) along with 2-(benzyloxy)-4-chloropyrimidine in a ratio of 75:25, respectively. This mixture was used directly in the next step and reacted with *N*-methylpiperazine to give **24a**, which was obtained pure following chromatography. After iodination with NIS to yield **25a** and further coupling with 3-aminobenzenethiol, **26a** was obtained. **27a–f** was then obtained by reaction of the appropriate acid chloride with **26a**. Phenyl-substituted analogue **27g** was obtained by a similar route used for compounds **27a–f**; however, the first step in the synthesis utilized a Suzuki coupling to install a phenyl group selectively onto the 4-position of **22** to yield **23b** (Scheme 3).

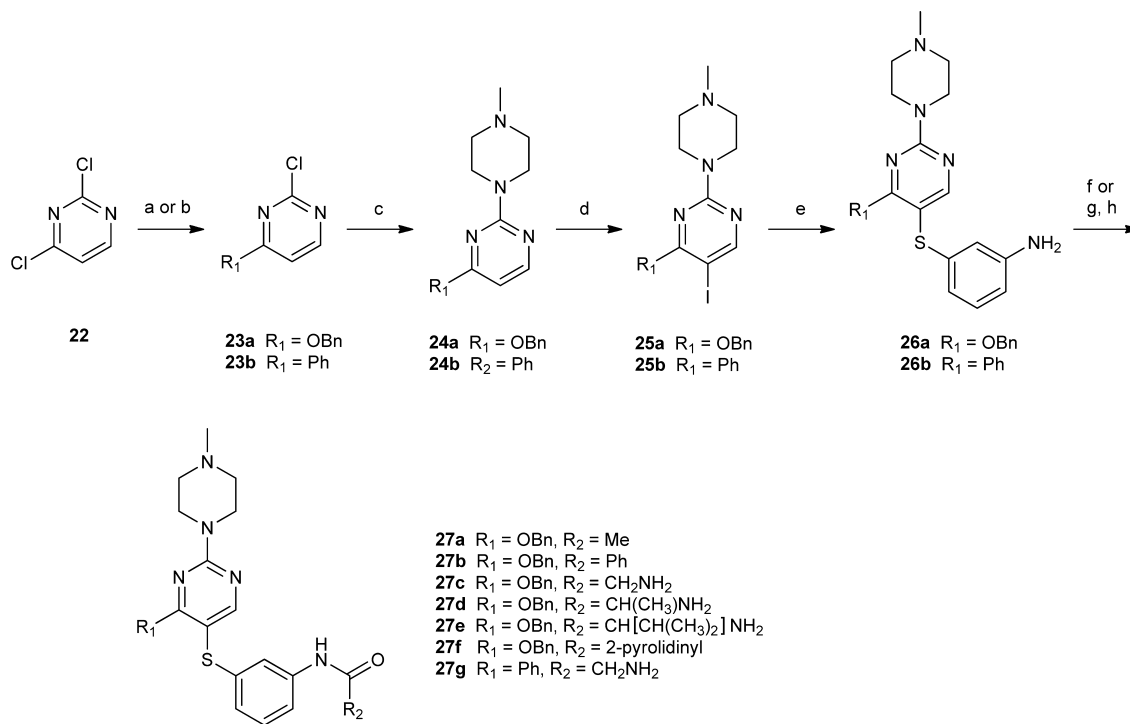
BIOLOGICAL EVALUATION AND STRUCTURE–ACTIVITY RELATIONSHIP IN THE HSP70 INHIBITOR SERIES

Our target-derived biological investigation was based on a specific battery of assays that we designed to probe Hsp70-derived mechanisms in a cancer cell.¹⁴ These include biochemical and phenotypic assays that probe biological effects that stem from alteration of the Hsp70–HOP–Hsp90 megacomplex and its chaperoning of oncoproteins.¹⁴ These biological tests were paralleled by computational studies, and each derivative was docked into the allosteric pocket of Hsp70 to understand the contribution of each chemical modification to the observed biological activity.

Our first step toward the potential realization of reversible inhibitors involved removing the reactive acrylamide moiety. Rewardingly, elimination of the covalent mode of binding by isosteric replacement of the acrylamide to ethylamide diminished the biological activity by only 1 log (i.e., **1a** vs **3a**, **1b** vs **4b**, **1c** vs **7a**, and **1d** vs **4c**, Tables 1 and 4) while retaining an Hsp70-driven mechanism of action (Table 1 and Figure 3). Specifically, when cancer cells were incubated with select derivatives (i.e., **1a** and **3a**, acrylamide- and ethylamide-

Scheme 2^a

^aReagents and conditions: (a) *N*-methylpiperazine, K_2CO_3 , DMF, 130 °C; (b) NIS, CH_3CN , rt; (c) 4-amino-2-mercaptopyrimidine, neocuproine, CuI , K_2CO_3 , DMF, 130 °C; (d) acid chloride, Et_3N , CH_2Cl_2 , rt; (e) 3-aminothiophenol, neocuproine, CuI , K_2CO_3 , DMF, 130 °C; (f) Boc-glycine, $EDCI$, $DMAP$, Et_3N , CH_2Cl_2 , rt, then TFA, rt; (g) 48% $HBr(aq)$, $(Bu)_4NBr$, reflux; (h) $(PMB)Cl$, NaH , DMF, rt.

Scheme 3^a

^aReagents and conditions: (a) $BnOH$, KOH , 18-crown-6, toluene, rt, 1 h; (b) $PhB(OH)_2$, Na_2CO_3 , $Pd(OAc)_2$, PPh_3 , DME, 95 °C, 15–20 h; (c) *N*-methylpiperazine, DMF, 80 °C, 1.75 h; (d) NIS, TFA, CH_3CN , rt, 1 h; (e) 3-aminobenzenethiol, neocuproine, CuI , K_2CO_3 or K_3PO_4 , DMF, 120 °C, 12–18 h; (f) Ac_2O , CH_2Cl_2 or $PhCOCl$, Et_3N , CH_2Cl_2 ; (g) $RCOOH$, DCC , THF, rt, 12 h; (h) CH_2Cl_2/TFA (4:1), rt.

Table 4^a

compd	HER2 ^b	Raf-1 ^b	cPARP ^b	growth inhibition ^b	Hsp90 binding ^c
1a	1	2.5	1.5	1.1	>500
1d	4	5	5	1.8	>500
3a	50	70	80	55	>250
7a	75	80	75	55	>500
3c	125	150	180	NA	>500
7b	18	20	18	15	>50
3d	>25	>25	>25	NA	>500
7e	7.5	10	7.5	8	497
7c	70	45	75	70	>250
4d	25	25	30	30	>250
7f	20	20	40	25	>500
9	70	50	75	ND	>500
16c	19	20	25	20	>250
7h	18	15	19	15	>500
27c	1.5	1.2	1.5	2.1	>500

^aAll values are in micromolar units. ^bHER2 and Raf-1 steady-state levels, PARP cleavage and inhibition of growth measured in SKBr3 breast cancer cells. ^cBinding to SKBr3 cell extracts tested at the maximum concentration allowed by solubility.

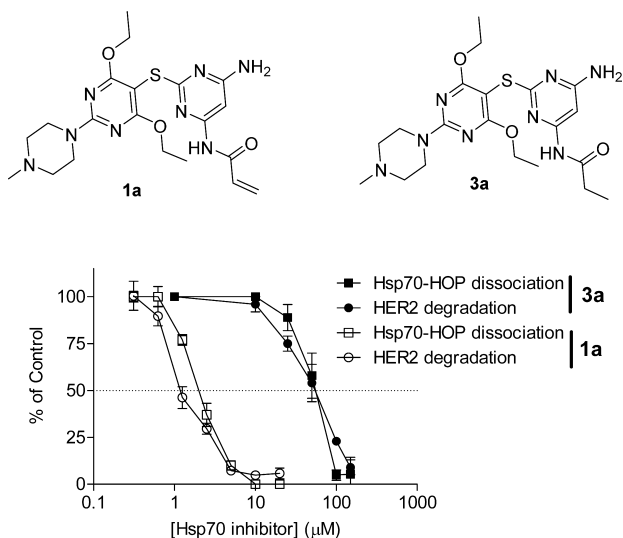


Figure 3. Hsp70–HOP dissociation and HER2 degradation by 1a and 3a. SKBr3 cells were treated for 24 h with vehicle or indicated concentrations of 1a or 3a. Hsp70–HOP dissociation: Upon cell lysing, Hsp70 complexes were isolated with an anti-Hsp70 antibody (IP BB70) and analyzed by Western blotting (WB). Specificity of binding was tested with a control IgG. HER2 degradation: Proteins in the lysate were analyzed by immunoblotting with an anti-HER2 antibody. β -Actin was used to control for equal loading. Gels were quantified by densitometry, values normalized to the control (vehicle only treated cells), and data graphed against the Hsp70 inhibitor concentration. Error bars represent the SD of the mean ($n = 3$).

containing derivatives, respectively), we observed dissociation of Hsp70–HOP complexes at concentrations at which we also noted degradation of the Hsp70 onco-client protein kinase, HER2 (Figure 3). As previously mentioned, HOP is a cochaperone that bridges Hsp70 and Hsp90 to form the megachaperone complex that regulates the stability of several onco-client proteins, such as HER2 and Raf-1. When these complexes become disrupted, the client proteins (i.e., HER2 and Raf-1) become unstable and are cleared through the proteasome pathway.¹⁵ As mentioned above, the pocket

occupied by the X₄ substituent contains Leu237, Val238, and Cys267, and the ethyl group of 3a would be well positioned to form hydrophobic interactions with these residues.

We wanted to explore the further potential of increasing potency by exploring this pocket with R groups of various sizes and to take advantage of potential hydrophobic interactions within the pocket. Substituting ethyl with methyl (i.e., 3c and 4a) diminished activity, while cyclopropyl at this position slightly increased activity (i.e., 4c vs 4e and 3a vs 7b, Table 1, X_{1,2} = N). Substitution of ethyl with groups such as allyl or cyclobutyl (i.e., 7a vs 7g and 7c) led to no significant change in activity, suggesting that such groups can be accommodated in this site, but that no additional favorable interactions were possible. Much larger hydrophobic substituents at this position abolished both activity (i.e., *n*-heptyl in 3d, steric clashes with Asn235, Leu237, Val238, and Val260¹⁵) and solubility (i.e., cyclohexyl in 7d), which in the latter case precluded biological evaluation.

We also found that flat, conformationally restricted aromatic groups were well tolerated at this position and in fact significantly improved activity. Specifically, the 2-furanyl derivative (i.e., 4d) was 2–3-fold more potent than the corresponding ethyl and cyclopropyl derivatives (i.e., 4c and 4e, respectively) and only 5-fold less potent than the corresponding acrylamide derivative (i.e., 1d) (Table 1). Even more favored was a phenyl at this position (i.e., 7e), this compound being 8–10-fold more active than the corresponding ethyl derivative (i.e., 7a) (Tables 1 and 4). Such an increase in potency for hydrophobic and π -electron-containing R groups may be explained by enhanced hydrophobic interactions with Leu237, Val238, Leu263, and Phe241 or a potential S– π interaction between the sulfur of Cys267 and the R group. Such favorable interactions between sulfur and π aromatic systems were first suggested by Morgan et al.,²⁶ and a number of stable orientations are possible, including one where the sulfur is positioned 3.5–4.0 Å above the plane of the aromatic ring and another where the sulfur is positioned slightly above (≤ 2.5 Å) and to the edge (4.5–6.0 Å) of the aromatic ring.²² Both orientations have been found to occur with cysteine residues in proteins, and recently a S–H/ π interaction was proposed to rationalize the binding affinity of an FLT3 kinase inhibitor.²⁷

Our second approach toward enhancing activity within the pocket was to take advantage of the native cysteine residue and its potential to form ionic interactions through its side chain thiolate (S[−]). We attempted to take advantage of such an interaction by incorporating an amine group at the same position as the β -carbon of the Michael acceptor acrylamide in 1a.^{28–30} An increase in potency was observed for R substituents that could potentially be positively ionized and form an ionic pair with S[−] of cysteine (2-aminomethyl in 7f and 16d). Indeed, 2-aminomethyl appears to favorably position its amine, which is likely protonated at physiological pH, to interact with the sulfur of cysteine (i.e., 7f in Table 1 and 16d in Table 2). These derivatives have an activity that is comparable to that of the corresponding phenyl and/or furanyl compounds (7f vs 7e and 4d, Table 1, and 16d vs 16c, Table 2). Positioning the amine one carbon away, such as in 9 (R = 2-(dimethylamino)-ethyl, Table 1), resulted in activity comparable to that of 7f in the growth inhibition and caspase-3,7 activation assays. In this case, 9 has the potential to undergo bioconversion in cells via β -elimination to the corresponding alkene,³¹ and therefore, in addition to possible interactions described above, it may also interact with Cys267 covalently.

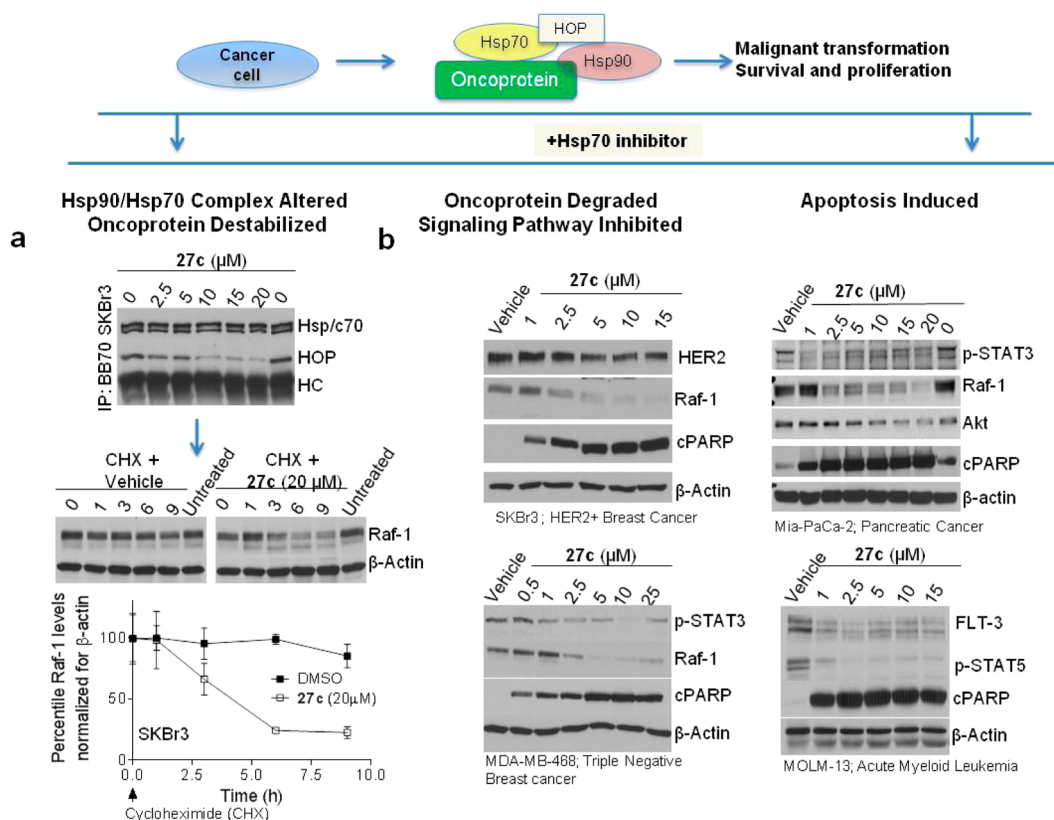


Figure 4. Allosteric ligands with a reversible mode of binding mimic the cellular phenotype observed with the irreversible Hsp70 inhibitors. Addition of 27c to cancer cells dose-dependently alters the formation of the Hsp70–HOP complex, a phenomenon associated with their destabilization and reduction in half-life (a). It is associated with degradation and/or inhibition of Hsp90–Hsp70 oncoproteins and induction of apoptosis (b). Collectively, these data indicate that its mechanism of action is mediated by interaction with the Hsp70 allosteric pocket in a fashion resembling the interaction of 1e.^{14,15}

Having determined these two potential strategies that replace the acrylamide with minimal loss of activity, i.e., a π -electron- or positively ionizable functionality-containing R group, we went on to explore other sites on the molecule that would provide a gain in binding affinity. As mentioned in our design, changing ring B from pyrimidine to phenyl is expected to increase potency by enhancing the interaction of the ring with Arg264. Indeed, unlike in the irreversible inhibitor series, where pyrimidine was favored over phenyl because it increased the reactivity of acrylamide for cysteine,¹⁴ in the reversible inhibitor series, we found the opposite to be true (i.e., 7a vs 4b and 16b vs 14b, Tables 1 and 2, and additional examples in Table 1). Changing ring B from pyrimidine to a phenyl improved the activity 2-fold. Arg264 has its guanidinium group positioned atop ring B, thus favorably aligned for cation– π interactions to occur (Figure 2a).¹⁹ Thus, an electron-rich aromatic ring, such as phenyl, may form a stronger stacking interaction than pyrimidine with this residue. In heterocycles, where the lone pair does not contribute to aromaticity, the electronegativity of the heteroatom weakens the cation– π binding ability.

We next explored modifications to ring A. Having ring A either pyrimidine or pyridine could increase the chemistry feasibility for exploring distinct X_5 and X_6 combinations on the molecules, and thus, we first explored the effect on activity by changing the nature of the ring. Rewardingly, a change from pyrimidine to pyridine led to no substantial change in activity (i.e., 7e vs 16c and 7f vs 16d, Tables 1 and 2). On the other hand, disrupting the aromaticity of ring A completely abolished activity (21, Table 2). 2-Hydroxypyridines undergo tautomer-

ism to give pyridones which can behave like amides and exist mainly as the “amide” tautomer in most solvents. The dramatic loss of activity observed upon replacing the methoxy group with a hydroxy group at X_5 hinted at the importance of this position for binding energy and demonstrates that this group makes significant interactions that are essential for the potency of these compounds.

Thus, having the ability to use both pyridine and pyrimidine as ring A increased our chemical versatility, and we next explored distinct $X_{5,6}$ combinations. Results with the pyridine series (Table 2) showed that disubstitution of X_5 and X_6 was not necessarily required as having a single methoxy group on the molecule performed as well as having two. This was also observed within the pyrimidine series, as 7h was of potency similar to that of its disubstituted analogue 7f (Table 1). We therefore sought to explore this position further, especially by adding aryl substituents that, as indicated above, would be poised to fill the hydrophobic pocket currently occupied by methoxy (Figure 2b, red circle). Substitution of X_5 with benzyloxy led to a remarkable 1 log increase in potency (compare 27a to 7a). In fact, this derivative was almost as potent as the corresponding acrylamide-containing derivative (compare 27a to 1c). We further increased the activity of this compound once the methyl (R on X_4 ; see Figure 2a) was substituted with a phenyl or aminomethyl (27b and 27c, respectively, Table 3), both favored X_4 substituents (Tables 1 and 2). With aminomethyl being favored at this position, we also probed whether adding hydrophobic bulk to this functionality could lead to a gain in affinity. As indicated

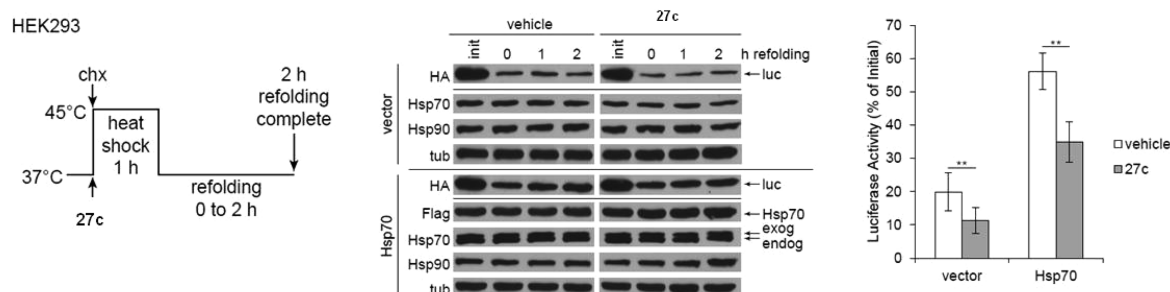


Figure 5. HEK2993 cells were transfected with luciferase and either control vector or Hsp70. The cells were treated with cycloheximide and either vehicle or 27c at 10 μ M, incubated at 45 $^{\circ}$ C for 1 h, and allowed to recover at 37 $^{\circ}$ C for 2 h (left). Cells were lysed during and after refolding, and soluble HA-tagged luciferase and chaperones were detected in the lysates; exogenous transfected Flag-tagged Hsp70 is visible as a band above endogenous Hsp70 (middle). Luciferase enzymatic activities in the lysates were measured at 2 h of refolding, unless otherwise indicated, and are represented as percentages of the initial activity before heat shock (right). 27c significantly inhibited endogenous Hsp70 and transfected Hsp70 in multiple experiments ($n \geq 3$).

above, Leu237 and Val238 are in the vicinity of Cys267, and thus, there is potential for minor affinity gain by increasing hydrophobicity. Replacing the H in 27c with a methyl (27d) or isopropyl (27e) or switching the aminomethyl to 2-pyrrolidinyl (27f) resulted in a minor increase in activity or had no measurable effect on activity (Table 3).

Changing X_5 from benzyloxy to the less flexible phenyl substituent directly attached to the pyrimidine A ring resulted in a significant 10-fold loss of activity (27g, Table 3). Furthermore, substituting the phenyl ring of 27c with the relatively more polar pyridine in 27h also decreased affinity 5-fold. These results are very much concordant with the proposed mode of binding for these ligands. Docking analysis showed that the benzyloxy group can be accommodated in the left-side hydrophobic subpocket (red circle, Figure 2b) and form hydrophobic interactions with Tyr41, Phe68, and Trp90. For 27g, the phenyl substituent is not able to orient properly in this cavity and, due to its inflexibility, rather orients toward Asp69 and Glu231, providing an explanation for its loss of activity. Similarly, replacing the phenyl in 27c with pyridine as in 27h increases the polarity and thus its ability to favorably interact with the hydrophobic residue environment.

Altogether, and as seen in the irreversible series, our tests demonstrated a good correlation between the predicted binding mode (Figure 2) and the observed biological activity (Tables 1–4) of the designed ligands, further consolidating that the biological effect of these molecules in cancer cells is majorly Hsp70 mediated. No effect was noted for these compounds on Hsp90 at concentrations as high as 500 μ M (Table 4).

One of the most active compounds derived from these studies is 27c. This ligand combines individual features that this study identifies as most favorable at each evaluated position; its X_4 is glycine, ring B is phenyl, and X_5 is benzyloxy (Figure 2b). This analogue has an activity in cells comparable to that of the most active reported irreversible inhibitors of this class,¹⁴ namely, low micromolar activity in cancer cells (Figure 4). We found that 27c interfered with the formation of functional Hsp70–HOP–Hsp90 machinery as indicated by its ability to dose-dependently alter the megacomplex components and to destabilize an Hsp70–Hsp90 machinery client, Raf-1 (Figure 4a). Hsp90 in concert with Hsp70 maintains the transforming capacity of several oncoproteins, including HER2, AKT, Raf-1, IGF-IR, and HIF-1.^{4,9} When this chaperone complex becomes pharmacologically inhibited, these oncoproteins become destabilized and are degraded mainly by the proteasomal pathway. Indeed, we found that the steady-state levels and/or

the activity of several oncoproteins involved in increased signaling through a pathogenic pathway were sensitive to Hsp70 inhibition by 27c (Figure 4b). These signaling oncoproteins include HER2 and Raf-1 in the HER2-over-expressing SKBr3 breast cancer cells, STAT3 and Raf-1 in the triple-negative breast cancer MDA-MB-468 cells, STAT3, Raf-1, and AKT in the MiaPaCa2 pancreatic cancer cells, and mutant FLT3 and STAT5 in MOLM13 acute myeloid leukemia cells. 27c also resulted in induction of apoptosis in these cancer cells, as indicated by substantial PARP cleavage (cPARP; Figure 4b).

Next, we investigated whether binding of 27c to Hsp70 interfered with its main biochemical activities, specifically refolding of a denatured client protein (Figure 5). Hsp70 activities are stimulated by Hsp40 proteins and nucleotide exchange factors, such as Hsp110.^{1,7,32} Humans have several cytosolic Hsp40's, including Hdj1, DJA1, DJA2, and DJA4, and it has recently been reported that DJA2 is most efficient in promoting the refolding of an Hsp70 polypeptide substrate, firefly luciferase.^{33–35} In cells, the refolding of heat-denatured luciferase by endogenous as well as transfected Hsp70 was inhibited by 27c. The nonspecific capacity of transfected Hsp70 to maintain substrate solubility after heat shock was not greatly affected, indicating that 27c, in a manner we reported for 1e,¹⁵ targeted the specific substrate folding activity of Hsp70 (Figure 5).

CONCLUSIONS

We have shown that significant biological activity may be retained through reversible Hsp70 inhibitors targeting an allosteric pocket located at the N-terminal domain. Because of the appropriate fit, and thus good enthalpy of binding of the irreversible inhibitors, simple modifications such as replacement of the covalent linkage with an ionic bridge (yellow, Figure 2b) and filling of the hydrophobic pocket occupied by methoxy in 1e with a benzyloxy (red, Figure 2b) have led to ligands of reversible mode of binding that not only mimic the phenotype observed with 1e, but do so with similar potency (Figure 4).

Our data show that the acrylamide group could be eliminated altogether by improving the enthalpy of the binding and indicate that significant binding energy can be attained through additional hydrophobic interactions of X_5 substituents with the Tyr41, Phe68, and Trp90 residues. This interaction weighs majorly toward the binding of these ligands to the allosteric pocket of Hsp70.

Combined, the SAR data from this and the accompanying paper¹⁴ validate the homology model and the proposed binding of these ligands to the allosteric pocket. First, the model has allowed for the rational design of a ligand that, when incubated with the thousands of proteins expressed in a cancer cell, affinity purified one, Hsp70. Second, the correctness of the binding mode analyses has allowed the rational design of specific ligands with a tractable SAR. Some of these specific ligands as we show have a reversible mode of binding whose potency rivals that of the irreversible ligands, indicating that favorable enthalpy drives the binding of these compounds to Hsp70. Third, the concordance in the observed biochemical and phenotypic effects observed with these agents in cancer cells, such as exemplified for **27c**, suggests that, in the tested concentration range, the biological activity of these agents is majorly and selectively channeled through an Hsp70-binding mechanism.

In addition to providing both a novel pharmacophore and medicinal chemistry for its assembly, we describe in our papers a testing battery for assessing Hsp70-mediated mechanisms in cancer cells and for evaluating specific ligand action in cancer cells through Hsp70 inhibition. Therefore, we provide a novel blueprint for a cancer-oriented development of Hsp70-directed ligands.

In conclusion, our findings propose the allosteric Hsp70 inhibitors as important leads toward the development of novel targeted anticancer therapeutics. **27c** serves as a molecule for further development that can potentially be elaborated into more potent molecules with in vivo efficacy. We are currently working to further optimize this class of compounds for potency and in vivo activity and will disclose our results in due course.

EXPERIMENTAL SECTION

Chemistry. All reagents were purchased from either Aldrich or Acros Organics and used without purification. All reactions were performed under argon protection. NMR spectra were recorded on a Bruker AV-III-500 or 600 MHz NMR spectrometer. Chemical shifts are reported in δ values in parts per million downfield from TMS as the internal standard. ¹H data are reported as follows: chemical shift, multiplicity (*s* = singlet, *d* = doublet, *t* = triplet, *q* = quartet, *br* = broad, *m* = multiplet), coupling constant (Hz), integration. ¹³C chemical shifts are reported in δ values in parts per million downfield from TMS as the internal standard. High-resolution mass spectra were recorded on a Waters LCT Premier system. Low-resolution mass spectra were obtained on a Waters Acquity Ultra Performance LC instrument with electrospray ionization and an SQ detector. Analytical HPLC was performed on a Waters Autopurification system with PDA, MicroMass ZQ, and ELSD detectors. The purity of the title compounds used in pharmacology testing was verified by HPLC–MS using the following method: 10–12 min gradient on a Waters2525 binary gradient pump of increasing concentrations of acetonitrile in water (5% → 95%) containing 0.1% formic acid with a flow rate of 1.2 mL/min and UV detection at λ = 220 and 254 nm on an XBridge C18 150 mm × 4.6 mm, 5 μ m column. Title compounds used in pharmacology testing were >95% pure. Analytical thin-layer chromatography was performed on 250 μ m silica gel F₂₅₄ plates. Preparative thin-layer chromatography was performed on 1000 μ m silica gel F₂₅₄ plates. Flash column chromatography was performed employing 230–400 mesh silica gel. Solvents were HPLC grade. The syntheses of **1a–d** and **8** are described elsewhere.¹⁴

N-(6-Amino-2-((4,6-diethoxy-2-(4-methylpiperazin-1-yl)pyrimidin-5-yl)thio)pyrimidin-4-yl)propionamide (**3a**). To a solution of **2a** (20 mg, 0.049 mmol) and Et₃N (49 mg, 0.49 mmol) in 1 mL of anhydrous dioxane was added propionyl chloride (45 mg, 0.49 mmol). The resulting mixture was stirred at rt for 12 h. Solvent was removed

under reduced pressure, and the residue was purified by preparatory TLC (CHCl₃/MeOH–NH₃ (7 N), 10:1) to afford 15 mg (66%) of **3a**. ¹H NMR (500 MHz, CDCl₃): δ 8.17 (br s, 1H), 6.95 (s, 1H), 4.84 (br s, 2H), 4.35 (q, *J* = 7.5, 4H), 3.82 (m, 4H), 2.44 (m, 4H), 2.34 (s, 3H), 2.34 (q, *J* = 7.5 Hz, 2H), 1.28 (t, *J* = 7.5 Hz, 6H), 1.15 (t, *J* = 7.5 Hz, 3H). ¹³C NMR (125 MHz, CDCl₃): δ 173.3, 170.6, 170.5, 164.2, 160.0, 156.7, 87.7, 80.3, 62.4, 54.9, 46.3, 43.7, 30.6, 14.5, 9.1. HRMS (*m/z*): [M + H]⁺ calcd for C₂₀H₃₁N₈O₃S, 463.2240; found, 463.2253.

N-(6-Amino-2-((4,6-diethoxy-2-(4-methylpiperazin-1-yl)pyrimidin-5-yl)thio)pyrimidin-4-yl)cyclopropanecarboxamide (**3b**). To a solution of **2a** (20 mg, 0.049 mmol) and Et₃N (49 mg, 0.49 mmol) in 1 mL of anhydrous dioxane was added cyclopropanecarbonyl chloride (62 mg, 0.49 mmol). The resulting mixture was stirred at rt for 12 h. Solvent was removed under reduced pressure, and the residue was purified by preparatory TLC (CHCl₃/MeOH–NH₃ (7 N), 10:1) to afford 23 mg (62%) of **3b**. ¹H NMR (500 MHz, CDCl₃): δ 8.48 (br s, 1H), 6.91 (s, 1H), 4.83 (br s, 2H), 4.35 (q, *J* = 7.1 Hz, 4H), 3.82 (m, 4H), 2.44 (m, 4H), 2.34 (s, 3H), 1.52 (m, 1H), 1.27 (t, *J* = 7.1 Hz, 6H), 1.03 (m, 2H), 0.84 (m, 2H). ¹³C NMR (125 MHz, CDCl₃): δ 173.3, 170.6, 170.5, 164.2, 160.0, 156.7, 87.8, 80.4, 62.5, 54.9, 46.3, 43.7, 15.9, 14.5, 8.7. HRMS (*m/z*): [M + H]⁺ calcd for C₂₁H₃₁N₈O₃S, 475.2240; found, 475.2237.

N-(6-Amino-2-((4,6-dimethoxy-2-(4-methylpiperazin-1-yl)pyrimidin-5-yl)thio)pyrimidin-4-yl)acetamide (**3c**). To a solution of **2b** (20 mg, 0.049 mmol) and Et₃N (49 mg, 0.49 mmol) in 1 mL of anhydrous dioxane was added acetyl chloride (38 mg, 0.49 mmol). The resulting mixture was stirred at rt for 12 h. Solvent was removed under reduced pressure, and the residue was purified by preparatory TLC (CHCl₃/MeOH–NH₃ (7 N), 10:1) to afford 21 mg (61%) of **3c**. ¹H NMR (500 MHz, CDCl₃): δ 7.99 (br s, 1H), 6.94 (s, 1H), 4.81 (br s, 2H), 3.88 (m, 10H), 2.47 (m, 4H), 2.36 (s, 3H), 2.11 (s, 3H). ¹³C NMR (125 MHz, CDCl₃): δ 171.1, 170.5, 169.3, 164.3, 160.1, 156.6, 87.8, 80.1, 54.9, 54.2, 46.2, 43.7, 24.8. HRMS (*m/z*): [M + H]⁺ calcd for C₁₇H₂₅N₈O₃S, 421.1770; found, 421.1765.

N-(6-Amino-2-((4,6-dimethoxy-2-(4-methylpiperazin-1-yl)pyrimidin-5-yl)thio)pyrimidin-4-yl)octanamide (**3d**). To a solution of **2b** (20 mg, 0.049 mmol) and Et₃N (49 mg, 0.49 mmol) in 1 mL of anhydrous dioxane was added octanoyl chloride (80 mg, 0.49 mmol). The resulting mixture was stirred at rt for 12 h. Solvent was removed under reduced pressure, and the residue was purified by preparatory TLC (CHCl₃/MeOH–NH₃ (7 N), 10:1) to afford 17 mg (71%) of **3d**. ¹H NMR (500 MHz, CDCl₃): δ 8.01 (br s, 1H), 6.97 (s, 1H), 4.86 (br s, 2H), 3.89 (s, 6H), 3.86 (m, 4H), 2.46 (m, 4H), 2.35 (s, 3H), 2.30 (t, *J* = 7.4 Hz, 2H), 1.62 (m, 2H), 1.20–1.30 (m, 8H), 0.87 (t, *J* = 6.9 Hz, 3H). ¹³C NMR (125 MHz, CDCl₃): δ 172.7, 171.1, 170.4, 164.3, 160.0, 156.7, 87.9, 80.1, 54.9, 54.2, 46.3, 43.7, 37.7, 31.6, 29.1, 29.0, 25.2, 22.6, 14.1. HRMS (*m/z*): [M + H]⁺ calcd for C₂₃H₃₇N₈O₃S, 505.2709; found, 505.2701.

N-(2-((4,6-Dimethoxy-2-(4-methylpiperazin-1-yl)pyrimidin-5-yl)thio)pyrimidin-4-yl)acetamide (**4a**). To a solution of **2c** (50 mg, 0.138 mmol) and Et₃N (139 mg, 1.38 mmol) in 2 mL of anhydrous dioxane was added acetyl chloride (108 mg, 1.38 mmol) dropwise. The resulting mixture was stirred at rt for 12 h. Solvent was removed under reduced pressure, and the residue was purified by preparatory TLC (CHCl₃/MeOH–NH₃ (7 N), 10:1) to afford 56 mg (73%) of **4a**. ¹H NMR (500 MHz, CDCl₃): δ 8.34 (d, *J* = 6.2 Hz, 1H), 8.09 (s, 1H), 7.75 (d, *J* = 6.2 Hz, 1H), 3.89 (br s, 10H), 2.50 (m, 4H), 2.38 (s, 3H), 2.18 (s, 3H). ¹³C NMR (125 MHz, CDCl₃): δ 171.4, 171.1, 169.3, 160.1, 158.9, 157.0, 105.4, 79.4, 54.8, 54.2, 46.2, 43.6, 24.8. HRMS (*m/z*): [M + H]⁺ calcd for C₁₇H₂₄N₇O₃S, 406.1661; found, 406.1661.

N-(2-((4,6-Dimethoxy-2-(4-methylpiperazin-1-yl)pyrimidin-5-yl)thio)pyrimidin-4-yl)propionamide (**4b**). To a solution of **2c** (50 mg, 0.138 mmol) and Et₃N (139 mg, 1.38 mmol) in 2 mL of anhydrous dioxane was added propionyl chloride (128 mg, 1.38 mmol) dropwise. The resulting mixture was stirred at rt for 12 h. Solvent was removed under reduced pressure, and the residue was purified by preparatory TLC (CHCl₃/MeOH–NH₃ (7 N), 10:1) to afford 58 mg (81%) of **4b**. ¹H NMR (500 MHz, CDCl₃): δ 8.33 (d, *J* = 5.6 Hz, 1H), 8.05 (s, 1H), 7.77 (d, *J* = 5.6 Hz, 1H), 3.96 (m, 4H), 3.89 (s, 6H), 2.59 (m,

4H), 2.42 (s, 3H), 2.41 (q, $J = 7.6$ Hz, 2H), 1.20 (t, $J = 7.6$ Hz, 3H). ^{13}C NMR (125 MHz, CDCl_3): δ 173.0, 171.2, 171.1, 160.1, 158.9, 157.0, 105.5, 77.0, 54.6, 54.3, 45.7, 43.1, 30.8, 9.0. HRMS (m/z): $[\text{M} + \text{H}]^+$ calcd for $\text{C}_{18}\text{H}_{26}\text{N}_7\text{O}_3\text{S}$, 420.1818; found, 420.1838.

N-(2-((4,6-Dimethyl-2-(4-methylpiperazin-1-yl)pyrimidin-5-yl)thio)pyrimidin-4-yl)propionamide (**4c**). To a solution of **2d** (50 mg, 0.151 mmol) and Et_3N (152 mg, 1.51 mmol) in 2 mL of anhydrous dioxane was added propionyl chloride (140 mg, 1.51 mmol) dropwise. The resulting mixture was stirred at rt for 12 h. Solvent was removed under reduced pressure, and the residue was purified by preparatory TLC ($\text{CHCl}_3/\text{MeOH}-\text{NH}_3$ (7 N), 10:1) to afford 59 mg (83%) of **4c**. ^1H NMR (500 MHz, CDCl_3): δ 8.35 (d, $J = 5.7$ Hz, 1H), 7.84 (s, 1H), 7.81 (d, $J = 5.7$ Hz, 1H), 3.92 (s, 4H), 2.48 (m, 4H), 2.44 (s, 6H), 2.40 (q, $J = 7.5$ Hz, 2H), 2.35 (s, 3H), 1.21 (t, $J = 7.5$ Hz, 3H). ^{13}C NMR (125 MHz, CDCl_3): δ 173.0, 171.9, 170.7, 160.4, 159.1, 157.3, 108.7, 105.7, 55.0, 46.2, 43.5, 30.8, 23.9, 8.9. HRMS (m/z): $[\text{M} + \text{H}]^+$ calcd for $\text{C}_{18}\text{H}_{26}\text{N}_7\text{OS}$, 388.1920; found, 388.1921.

N-(2-((4,6-Dimethyl-2-(4-methylpiperazin-1-yl)pyrimidin-5-yl)thio)pyrimidin-4-yl)furan-2-carboxamide (**4d**). To a solution of **2d** (50 mg, 0.151 mmol) and Et_3N (152 mg, 1.51 mmol) in 2 mL of anhydrous dioxane was added 2-furoyl chloride (197 mg, 1.51 mmol) dropwise. The resulting mixture was stirred at rt for 12 h. Solvent was removed under reduced pressure, and the residue was purified by preparatory TLC ($\text{CHCl}_3/\text{MeOH}-\text{NH}_3$ (7 N), 10:1) to afford 56 mg (87%) of **4d**. ^1H NMR (600 MHz, CDCl_3): δ 8.58 (br s, 1H), 8.40 (d, $J = 5.6$ Hz, 1H), 7.94 (d, $J = 5.6$ Hz, 1H), 7.56–7.58 (m, 1H), 7.31 (d, $J = 3.5$ Hz, 1H), 6.60 (dd, $J = 3.5, 1.7$ Hz, 1H), 3.90–3.97 (m, 4H), 2.49 (m, 4H), 2.46 (s, 6H), 2.36 (s, 3H). ^{13}C NMR (150 MHz, CDCl_3): δ 171.9, 170.9, 160.5, 159.1, 157.1, 156.3, 146.4, 145.4, 117.2, 113.0, 108.5, 106.0, 55.0, 46.3, 43.5, 23.9. HRMS (m/z): $[\text{M} + \text{H}]^+$ calcd for $\text{C}_{20}\text{H}_{24}\text{N}_7\text{O}_2\text{S}$, 426.1712; found, 426.1727.

N-(2-((4,6-Dimethyl-2-(4-methylpiperazin-1-yl)pyrimidin-5-yl)thio)pyrimidin-4-yl)cyclopropanecarboxamide (**4e**). To a solution of **2d** (50 mg, 0.151 mmol) and Et_3N (152 mg, 1.51 mmol) in 2 mL of anhydrous dioxane was added cyclopropanecarbonyl chloride (158 mg, 1.51 mmol) dropwise. The resulting mixture was stirred at rt for 12 h. Solvent was removed under reduced pressure, and the residue was purified by preparatory TLC ($\text{CHCl}_3/\text{MeOH}-\text{NH}_3$ (7 N), 10:1) to afford 48 mg (79%) of **4e**. ^1H NMR (500 MHz, CDCl_3): δ 8.35 (d, $J = 5.6$ Hz, 1H), 8.20 (s, 1H), 7.78 (d, $J = 5.6$ Hz, 1H), 3.92 (m, 4H), 2.49 (m, 4H), 2.45 (s, 6H), 2.36 (s, 3H), 1.54 (m, 1H), 1.10 (m, 2H), 0.93 (m, 2H). ^{13}C NMR (125 MHz, CDCl_3): δ 173.1, 172.0, 170.6, 160.4, 159.0, 157.3, 108.8, 105.7, 55.0, 46.2, 43.5, 23.8, 16.0, 9.1. HRMS (m/z): $[\text{M} + \text{H}]^+$ calcd for $\text{C}_{19}\text{H}_{26}\text{N}_7\text{OS}$, 400.1920; found, 400.1913.

3-((4,6-Dimethoxy-2-(4-methylpiperazin-1-yl)pyrimidin-5-yl)thio)aniline (**6a**). A mixture of **5a** (0.200 g, 0.549 mmol), 3-aminothiophenol (70 μL , 0.082 g, 0.659 mmol), neocuproine (0.023 g, 0.110 mmol), CuI (0.021, 0.110 mmol), and K_2CO_3 (0.152 g, 1.10 mmol) in DMF (7 mL) was heated at 120 $^\circ\text{C}$ for 24 h. Solvent was removed under reduced pressure, and the residue was purified by column chromatography ($\text{CH}_2\text{Cl}_2/\text{MeOH}-\text{NH}_3$ (7 N), 200:1 to 40:1) to afford 0.133 g (67%) of **6a**. ^1H NMR (500 MHz, CDCl_3): δ 6.97 (t, $J = 8.0$ Hz, 1H), 6.46–6.51 (m, 1H), 6.36–6.40 (m, 2H), 3.88–4.03 (m, 10H), 3.58 (br s, 2H), 2.52 (m, 4H), 2.38 (s, 3H). ^{13}C NMR (125 MHz, CDCl_3): δ 171.8, 160.1, 146.9, 139.5, 129.6, 116.2, 112.2, 112.1, 81.1, 55.0, 54.6, 46.3, 43.8. HRMS (m/z): $[\text{M} + \text{H}]^+$ calcd for $\text{C}_{17}\text{H}_{24}\text{N}_5\text{O}_2\text{S}$, 362.1651; found, 362.1649.

N-(3-((4,6-Dimethoxy-2-(4-methylpiperazin-1-yl)pyrimidin-5-yl)thio)phenyl)propionamide (**7a**). To a solution of **6a** (10 mg, 0.027 mmol) and Et_3N (50 μL , 36 mg, 0.36 mmol) in 1 mL of CH_2Cl_2 was added propionyl chloride (22 μL , 24.4 mg, 0.27 mmol). The reaction was stirred at rt for 12 h and then quenched by adding cold MeOH. Solvent was evaporated under reduced pressure, and the residue was purified by preparatory TLC ($\text{CH}_2\text{Cl}_2/\text{MeOH}-\text{NH}_3$ (7 N), 20:1) to afford 7.3 mg (65%) of **7a**. ^1H NMR (500 MHz, CDCl_3): δ 7.44 (d, $J = 7.5$ Hz, 1H), 7.13 (m, 2H), 7.04 (s, 1H), 6.78 (d, $J = 7.5$ Hz, 1H), 3.93 (m, 4H), 3.90 (s, 6H), 2.55 (m, 4H), 2.36 (s, 3H), 2.33 (q, $J = 7.2$ Hz, 2H), 1.21 (t, $J = 7.2$ Hz, 3H). HRMS (m/z): $[\text{M} + \text{H}]^+$ calcd for $\text{C}_{20}\text{H}_{28}\text{N}_5\text{O}_3\text{S}$, 418.1913; found, 418.1910.

N-(3-((4,6-Dimethoxy-2-(4-methylpiperazin-1-yl)pyrimidin-5-yl)thio)phenyl)cyclopropanecarboxamide (**7b**). To a solution of **6a** (10.9 mg, 0.0302 mmol) and Et_3N (21 μL , 15.3 mg, 0.151 mmol) in CH_2Cl_2 (1 mL) was added cyclopropanecarbonyl chloride (14 μL , 15.8 mg, 0.1508 mmol), and the resulting solution was stirred at rt for 2 h. Solvent was removed under reduced pressure, and the residue was purified by preparatory TLC ($\text{CH}_2\text{Cl}_2/\text{MeOH}-\text{NH}_3$ (7 N), 20:1) to afford 7.9 mg (61%) of **7b**. ^1H NMR (500 MHz, CDCl_3): δ 7.49 (m, 1H), 7.29 (s, 1H), 7.13 (t, $J = 7.8$ Hz, 1H), 6.97 (s, 1H), 6.78 (d, $J = 7.6$ Hz, 1H), 3.88–3.95 (m, 10H), 2.48 (m, 4H), 2.36 (s, 3H), 1.05–1.13 (m, 1H), 0.74–0.96 (m, 4H). HRMS (m/z): $[\text{M} + \text{H}]^+$ calcd for $\text{C}_{21}\text{H}_{28}\text{N}_5\text{O}_3\text{S}$, 430.1913; found, 430.1897.

N-(3-((4,6-Dimethoxy-2-(4-methylpiperazin-1-yl)pyrimidin-5-yl)thio)phenyl)cyclobutanecarboxamide (**7c**). **6a** (10 mg, 0.028 mmol), Et_3N (19.5 μL , 14.2 mg, 0.14 mmol), and cyclobutanecarbonyl chloride (9.6 μL , 10.0 mg, 0.084 mmol) in CH_2Cl_2 (1 mL) were stirred at rt for 2 h. Solvent was removed under reduced pressure, and the residue was purified by preparatory TLC ($\text{EtOAc}/\text{MeOH}-\text{NH}_3$ (7 N), 20:1) to afford 4.1 mg (33%) of **7c**. ^1H NMR (500 MHz, CDCl_3): δ 7.50 (d, $J = 7.8$ Hz, 1H), 7.14 (t, $J = 7.9$ Hz, 1H), 7.00 (s, 1H), 6.94 (br s, 1H), 6.77 (d, $J = 7.9$ Hz, 1H), 3.90 (br s, 10H), 3.07 (m, 1H), 2.50 (m, 14H), 2.14–2.42 (m, 7H), 1.82–2.02 (m, 2H). HRMS (m/z): $[\text{M} + \text{H}]^+$ calcd for $\text{C}_{22}\text{H}_{30}\text{N}_5\text{O}_3\text{S}$, 444.2069; found, 444.2052.

N-(3-((4,6-Dimethoxy-2-(4-methylpiperazin-1-yl)pyrimidin-5-yl)thio)phenyl)cyclohexanecarboxamide (**7d**). **6a** (10 mg, 0.028 mmol), Et_3N (19.5 μL , 14.2 mg, 0.14 mmol), and cyclohexanecarbonyl chloride (11.4 μL , 12.3 mg, 0.084 mmol) in CH_2Cl_2 (1 mL) were stirred at rt for 3 h. Solvent was removed under reduced pressure, and the residue was purified by preparatory TLC ($\text{EtOAc}/\text{MeOH}-\text{NH}_3$ (7 N), 20:1) to afford 12 mg (91%) of **7d**. ^1H NMR (500 MHz, CDCl_3): δ 7.50 (d, $J = 7.9$ Hz, 1H), 7.18 (s, 1H), 7.13 (t, $J = 7.9$ Hz, 1H), 7.02 (s, 1H), 6.76 (d, $J = 7.7$ Hz, 1H), 3.90 (br s, 10H), 2.51 (m, 4H), 2.38 (s, 3H), 2.11–2.22 (m, 1H), 1.19–1.96 (m, 10H). MS (m/z): $[\text{M} + \text{H}]^+$ 472.0.

N-(3-((4,6-Dimethoxy-2-(4-methylpiperazin-1-yl)pyrimidin-5-yl)thio)phenyl)benzamide (**7e**). **6a** (10 mg, 0.028 mmol), Et_3N (19.5 μL , 14.2 mg, 0.14 mmol), and benzoyl chloride (9.8 μL , 11.8 mg, 0.084 mmol) in CH_2Cl_2 (1 mL) were stirred at rt for 3 h. Solvent was removed under reduced pressure, and the residue was purified by preparatory TLC ($\text{EtOAc}/\text{MeOH}-\text{NH}_3$ (7 N), 20:1) to afford 8.6 mg (66%) of **7e**. ^1H NMR (500 MHz, CDCl_3): δ 7.83 (d, $J = 7.7$ Hz, 2H), 7.74 (br s, 1H), 7.59 (d, $J = 7.8$ Hz, 1H), 7.54 (t, $J = 6.4$ Hz, 1H), 7.47 (t, $J = 7.8$ Hz, 2H), 7.20 (t, $J = 8.0$ Hz, 1H), 7.13 (s, 1H), 6.86 (d, $J = 7.9$ Hz, 1H), 3.87–3.93 (m, 10H), 2.50 (m, 4H), 2.37 (s, 3H). HRMS (m/z): $[\text{M} + \text{H}]^+$ calcd for $\text{C}_{24}\text{H}_{28}\text{N}_5\text{O}_3\text{S}$, 466.1913; found, 466.1919.

2-Amino-*N*-(3-((4,6-dimethoxy-2-(4-methylpiperazin-1-yl)pyrimidin-5-yl)thio)phenyl)acetamide (**7f**). To a solution of **6a** (20 mg, 0.0552 mmol) in THF (1 mL) were added Boc-glycine (9.7 mg, 0.0552 mmol) and DCC (12 mg, 0.058 mmol), and the resulting solution was stirred at rt for 5 h. The reaction mixture was concentrated under reduced pressure, and the residue was purified by preparatory TLC ($\text{EtOAc}/\text{MeOH}-\text{NH}_3$ (7 N), 20:1) to afford a solid which was dissolved in 2 mL of $\text{CH}_2\text{Cl}_2/\text{TFA}$ (4:1). The resulting solution was stirred at rt for 1 h. The reaction mixture was concentrated under reduced pressure, and the residue was purified by preparatory TLC ($\text{CH}_2\text{Cl}_2/\text{MeOH}-\text{NH}_3$ (7 N), 15:1) to afford 13.9 mg (60%) of **7f**. ^1H NMR (500 MHz, $\text{CDCl}_3/\text{MeOH}-d_4$): δ 7.38 (d, $J = 8.2$ Hz, 1H), 7.26 (s, 1H), 7.15 (t, $J = 7.9$ Hz, 1H), 6.79 (d, $J = 7.6$ Hz, 1H), 3.86–3.97 (m, 10H), 3.52 (s, 2H), 2.58 (m, 4H), 2.41 (s, 3H). HRMS (m/z): $[\text{M} + \text{H}]^+$ calcd for $\text{C}_{19}\text{H}_{27}\text{N}_6\text{O}_3\text{S}$, 419.1865; found, 419.1862.

N-(3-((4,6-Dimethoxy-2-(4-methylpiperazin-1-yl)pyrimidin-5-yl)thio)phenyl)but-3-enamide (**7g**). To a solution of **6a** (10 mg, 0.027 mmol) and Et_3N (50 μL , 36 mg, 0.36 mmol) in 1 mL of CH_2Cl_2 was added 3-butenoyl chloride (28.2 mg, 0.27 mmol). The reaction was stirred at rt for 12 h and then quenched by adding cold MeOH. Solvent was evaporated under reduced pressure, and the residue was purified by preparatory TLC ($\text{CH}_2\text{Cl}_2/\text{MeOH}-\text{NH}_3$ (7 N), 20:1) to afford 8.3 mg (72%) of **7g**. ^1H NMR (500 MHz, CDCl_3): δ 7.35 (d, $J = 8.1$ Hz, 1H), 7.29 (br s, 1H), 7.10–7.19 (m, 2H), 6.79 (d, $J = 7.5$

H₂, 1H), 5.97–6.00 (m, 1H), 5.25–5.35 (m, 2H), 3.92–3.96 (m, 4H), 3.90 (s, 6H), 3.14 (d, *J* = 7.1 Hz, 2H), 2.54–2.60 (m, 4H), 2.42 (s, 3H). HRMS (*m/z*): [M + H]⁺ calcd for C₂₁H₂₈N₅O₃S, 430.1913; found, 430.1911.

3-((4-Methoxy-2-(4-methylpiperazin-1-yl)pyrimidin-5-yl)thio)aniline (6b). A mixture of **5b** (0.200 g, 0.600 mmol) and K₂CO₃ (0.166 g, 1.20 mmol) in DMF (6 mL) was evacuated and backfilled with argon three times. Copper(I) thiophene-2-carboxylate (0.034 g, 0.180 mmol) was added, and the resulting mixture was evacuated and backfilled with argon two times. 3-Aminothiophenol (76 μL, 0.090 g, 0.72 mmol) was added, and the reaction mixture was heated at 120 °C for 24 h. Solvent was removed under reduced pressure, and the residue was purified by column chromatography (CH₂Cl₂/MeOH–NH₃ (7 N), 200:1 to 40:1) to afford 0.147 g (74%) of **6b**. ¹H NMR (500 MHz, CDCl₃): δ 8.22 (s, 1H), 7.00 (t, *J* = 7.8 Hz, 1H), 6.52 (d, *J* = 7.7 Hz, 1H), 6.38–6.45 (m, 2H), 3.91 (s, 3H), 3.89 (m, 4H), 3.60 (br s, 2H), 2.49 (m, 4H), 2.36 (s, 3H). ¹³C NMR (125 MHz, CDCl₃): δ 169.4, 164.9, 161.6, 146.9, 138.8, 129.6, 116.9, 112.9, 112.5, 99.2, 54.9, 53.9, 46.2, 43.8. HRMS (ESI) (*m/z*) [M + H]⁺ calcd for C₁₆H₂₂N₅O₃S, 332.1545; found, 332.1532.

2-Amino-N-(3-((4-methoxy-2-(4-methylpiperazin-1-yl)pyrimidin-5-yl)thio)phenyl)acetamide (7h). To a solution of **6b** (15.5 mg, 0.047 mmol) in THF (1 mL) were added Boc-glycine (9.1 mg, 0.052 mmol) and DCC (10.7 mg, 0.052 mmol). After the resulting solution was stirred overnight at rt, THF was evaporated and 1 mL of CH₂Cl₂/TFA (4:1) was added. The solution was stirred for 45 min and then concentrated to dryness under reduced pressure to give a residue which was purified by preparatory TLC (CH₂Cl₂/MeOH–NH₃ (7 N), 15:1) to afford 13.4 mg (73%) of **7h**. ¹H NMR (500 MHz, CDCl₃): δ 9.29 (br s, 1H), 8.23 (s, 1H), 7.45–7.50 (m, 1H), 7.30–7.34 (m, 1H), 7.17 (t, *J* = 8.0 Hz, 1H), 6.81–6.87 (m, 1H), 3.91 (s, 3H), 3.86–3.90 (m, 4H), 3.45 (s, 2H), 2.46–2.52 (m, 4H), 2.35 (s, 3H). MS (*m/z*): [M + H]⁺ 389.3.

N-(6-Amino-2-((4,6-dimethoxy-2-(4-methylpiperazin-1-yl)pyrimidin-5-yl)thio)pyrimidin-4-yl)-3-(dimethylamino)propanamide (9). To a solution of **8** (23 mg, 0.053 mmol) in CH₃CN (1 mL) were added dimethylamine (2 M, THF; 53 μL, 0.106 mmol) and DBU (4 mg, 0.026 mmol) at rt, and the resulting solution was stirred for 6 h. The reaction mixture was concentrated under reduced pressure, and the residue was purified by preparatory TLC (CH₂Cl₂/MeOH–NH₃ (7 N), 10:1) to afford 13.5 mg (53%) of **9**. ¹H NMR (600 MHz, CDCl₃): δ 11.1 (br s, 1H), 6.91 (s, 1H), 4.79 (br s, 2H), 3.84–3.91 (m, 10H), 2.56 (t, *J* = 5.8 Hz, 2H), 2.45–2.51 (m, 4H), 2.41 (t, *J* = 5.8 Hz, 2H), 2.37 (s, 3H), 2.22 (s, 6H). ¹³C NMR (150 MHz, CDCl₃): δ 171.9, 171.2, 170.2, 164.3, 160.0, 157.1, 88.4, 80.8, 54.9, 54.4, 54.1, 46.2, 44.1, 43.6, 33.6. HRMS (*m/z*): [M + H]⁺ calcd for C₂₀H₃₂N₉O₃S, 478.2349; found, 478.2343.

1-(6-Methoxypyridin-2-yl)-4-methylpiperazine (11). To a solution of 2-bromo-6-methoxypyridine (**10**) (150 mg, 0.8 mmol) and 1-methylpiperazine (240 mg, 2.4 mmol) in 2 mL of DMF was added of K₂CO₃ (220 mg, 1.6 mmol), and the resulting mixture was heated to 130 °C for 16 h. Solvent was evaporated under reduced pressure, and the residue was purified by column chromatography (5–10% MeOH in CH₂Cl₂) to afford 145 mg (88%) of **11**. ¹H NMR (500 MHz, CDCl₃): δ 7.41 (t, *J* = 8.0 Hz, 1H), 6.16 (d, *J* = 8.0 Hz, 1H), 6.08 (d, *J* = 8.0 Hz, 1H), 3.87 (s, 3H), 3.54 (m, 4H), 2.51 (m, 4H), 2.54 (s, 3H). ¹³C NMR (125 MHz, CDCl₃): δ 163.1, 158.3, 140.1, 98.2, 98.1, 54.8, 52.9, 46.2, 45.1. MS (*m/z*): [M + H]⁺ 208.4.

1-(5-Iodo-6-methoxypyridin-2-yl)-4-methylpiperazine (12). To a solution of **11** (124 mg, 0.6 mmol) in 5 mL of acetonitrile was added *N*-iodosuccinimide (203 mg, 0.9 mmol), and the resulting mixture was stirred at rt for 2 h. The solvent was evaporated under reduced pressure, and the residue was purified by column chromatography (CH₂Cl₂/MeOH–NH₃ (7 N), 1:0 to 85:15) to afford 190 mg (95%) of **12**. ¹H NMR (500 MHz, CDCl₃): δ 7.70 (d, *J* = 8.0 Hz, 1H), 6.02 (d, *J* = 8.0 Hz, 1H), 3.90 (s, 3H), 3.60 (m, 4H), 2.62 (m, 4H), 2.39 (s, 3H). ¹³C NMR (125 MHz, CDCl₃): δ 177.7, 160.5, 157.8, 148.6, 100.7, 61.7, 54.2, 45.5, 44.5. MS (*m/z*): [M + H]⁺ 334.1.

2-((2-Methoxy-6-(4-methylpiperazin-1-yl)pyridin-3-yl)thio)pyrimidin-4-amine (13). A mixture of **12** (100 mg, 0.3 mmol), 4-

aminopyrimidine-2-thiol (39 mg, 0.3 mmol), K₂CO₃ (83 mg, 0.6 mmol), neocuproine (11 mg, 0.05 mmol), and CuI (10 mg, 0.05 mmol) in DMF (3 mL) was heated to 130 °C for 16 h. Solvent was removed under reduced pressure, and the residue was purified by column chromatography (CH₂Cl₂/MeOH–NH₃ (7 N), 1:0 to 85:15) to afford 60 mg (60%) of **13**. ¹H NMR (500 MHz, CDCl₃): δ 7.95 (d, *J* = 8.0 Hz, 1H), 7.59 (d, *J* = 8.5 Hz, 1H), 6.20 (d, *J* = 8.5 Hz, 1H), 6.05 (d, *J* = 8.0 Hz, 1H), 5.01 (s, 2H), 3.87 (s, 3H), 3.62 (m, 4H), 2.54 (m, 4H), 2.36 (s, 3H). ¹³C NMR (125 MHz, CDCl₃): δ 171.9, 162.9, 162.5, 158.6, 156.2, 147.8, 101.1, 98.6, 97.6, 54.6, 53.6, 46.0, 44.6. MS (*m/z*): [M + H]⁺ 333.5.

N-(2-((2-Methoxy-6-(4-methylpiperazin-1-yl)pyridin-3-yl)thio)pyrimidin-4-yl)propionamide (14a). To a solution of **13** (20 mg, 0.06 mmol) in 1.5 mL of CH₂Cl₂ and Et₃N (100 μL) was added propionyl chloride in CH₂Cl₂ dropwise. Upon completion (by TLC), the reaction was quenched by adding cold MeOH. Solvent was removed under reduced pressure, and the residue was purified by column chromatography (MeOH–NH₃ (7 N), 2–10% in CH₂Cl₂) to afford 18 mg (80%) of **14a**. ¹H NMR (500 MHz, CDCl₃): δ 8.53 (br s, 1H), 8.34 (d, *J* = 8.0 Hz, 1H), 7.79 (d, *J* = 8.0 Hz, 1H), 7.58 (d, *J* = 8.0 Hz, 1H), 6.21 (d, *J* = 8.0 Hz, 1H), 3.86 (s, 3H), 3.63 (m, 4H), 2.52 (m, 4H), 2.41 (q, *J* = 7.2 Hz, 2H), 2.36 (s, 3H), 1.08 (t, *J* = 7.2 Hz, 3H). ¹³C NMR (125 MHz, CDCl₃): δ 173.4, 172.2, 171.7, 162.9, 158.8, 157.3, 147.6, 105.6, 98.7, 96.7, 54.6, 53.7, 46.0, 44.6, 30.6, 8.96. HRMS (*m/z*): [M + H]⁺ calcd for C₁₈H₂₅N₆O₂S, 389.1760; found, 389.1751.

N-(2-((2-Methoxy-6-(4-methylpiperazin-1-yl)pyridin-3-yl)thio)pyrimidin-4-yl)cyclopropanecarboxamide (14b). To a solution of **13** (20 mg, 0.06 mmol) in 1.5 mL of CH₂Cl₂ and Et₃N (100 μL) was added cyclopropanecarbonyl chloride in CH₂Cl₂ dropwise. Upon completion (by TLC), the reaction was quenched by adding cold MeOH. Solvent was removed under reduced pressure, and the residue was purified by column chromatography (MeOH–NH₃ (7 N), 2–10% in CH₂Cl₂) to afford 21 mg (90%) of **14b**. ¹H NMR (500 MHz, CDCl₃): δ 8.87 (br s, 1H), 8.31 (d, *J* = 8.0 Hz, 1H), 7.75 (d, *J* = 8.0 Hz, 1H), 7.57 (d, *J* = 8.0 Hz, 1H), 6.20 (d, *J* = 8.0 Hz, 1H), 3.87 (s, 3H), 3.62 (m, 4H), 2.52 (m, 4H), 2.36 (s, 3H), 1.61 (m, 1H), 1.08 (m, 2H), 0.88 (m, 2H). ¹³C NMR (125 MHz, CDCl₃): δ 176.4, 173.5, 171.7, 162.9, 158.8, 157.2, 147.6, 105.7, 98.6, 96.7, 54.7, 53.6, 46.1, 44.6, 14.0, 7.7. HRMS (*m/z*): [M + H]⁺ calcd for C₁₉H₂₅N₆O₂S, 401.1760; found, 401.1767.

3-((2-Methoxy-6-(4-methylpiperazin-1-yl)pyridin-3-yl)thio)aniline (15). A mixture of **12** (100 mg, 0.3 mmol), 3-aminothiophenol (37 mg, 0.3 mmol), K₂CO₃ (83 mg, 0.6 mmol), neocuproine (33 mg, 0.15 mmol), and CuI (29 mg, 0.15 mmol) in DMF (3 mL) was heated to 130 °C for 16 h. Solvent was removed under reduced pressure, and the residue was purified by column chromatography (CH₂Cl₂/MeOH–NH₃ (7 N), 1:0 to 90:10) to afford 60 mg (60%) of **15**. MS (*m/z*): [M + H]⁺ 331.2.

N-(3-((2-Methoxy-6-(4-methylpiperazin-1-yl)pyridin-3-yl)thio)phenyl)propionamide (16a). To a solution of **15** (20 mg, 0.06 mmol) and Et₃N (100 μL) in 1.5 mL of CH₂Cl₂ was added propionyl chloride in CH₂Cl₂ dropwise. Upon completion (by TLC), the reaction was quenched by adding cold MeOH. Solvent was removed under reduced pressure, and the residue was purified by column chromatography (MeOH–NH₃ (7 N), 2–10% in CH₂Cl₂) to afford 15 mg (70%) of **16a**. ¹H NMR (500 MHz, CDCl₃): δ 7.55 (d, *J* = 8.0 Hz, 1H), 7.45 (d, *J* = 8.0 Hz, 1H), 7.22 (br s, 1H), 7.14 (t, *J* = 8.0 Hz, 1H), 7.08 (s, 1H), 6.81 (d, *J* = 8.0 Hz, 1H), 6.20 (d, *J* = 8.0 Hz, 1H), 3.88 (s, 3H), 3.47 (m, 4H), 2.57 (m, 4H), 2.36 (s, 3H), 2.33 (q, *J* = 7.2 Hz, 2H), 1.19 (t, *J* = 7.2 Hz, 3H). HRMS (*m/z*): [M + H]⁺ calcd for C₂₀H₂₇N₄O₂S, 387.1855; found, 387.1855.

N-(3-((2-Methoxy-6-(4-methylpiperazin-1-yl)pyridin-3-yl)thio)phenyl)cyclopropanecarboxamide (16b). To a solution of **15** (20 mg, 0.06 mmol) and Et₃N (100 μL) in 1.5 mL of CH₂Cl₂ was added cyclopropanecarbonyl chloride in CH₂Cl₂ dropwise. Upon completion (by TLC), the reaction was quenched by adding cold MeOH. Solvent was removed under reduced pressure, and the residue was purified by column chromatography (MeOH–NH₃ (7 N), 2–10% in CH₂Cl₂) to afford 16 mg (70%) of **16b**. ¹H NMR (500 MHz, CDCl₃) δ 7.61 (s, 1H), 7.31 (d, *J* = 8.0 Hz, 1H), 7.20 (br s, 1H), 6.88 (m, 2H), 6.55 (m,

1H), 5.95 (d, $J = 8.0$ Hz, 1H), 3.63 (s, 3H), 3.37 (m, 4H), 2.29 (m, 4H), 2.09 (s, 3H), 1.25 (m, 1H), 0.78 (m, 2H), 0.57 (m, 2H). ^{13}C NMR (125 MHz, CDCl_3) δ 176.4, 172.1, 162.7, 158.4, 147.5, 139.3, 138.7, 129.2, 122.2, 117.5, 116.8, 99.0, 54.6, 53.6, 46.1, 44.7, 13.9, 7.9. HRMS (m/z): $[\text{M} + \text{H}]^+$ calcd for $\text{C}_{21}\text{H}_{27}\text{N}_4\text{O}_2\text{S}$, 399.1855; found, 399.1853.

N-(3-((2-Methoxy-6-(4-methylpiperazin-1-yl)pyridin-3-yl)thio)phenyl)benzamide (16c). To a solution of 15 (20 mg, 0.06 mmol) and Et_3N (100 μL) in 1.5 mL of CH_2Cl_2 was added benzoyl chloride in CH_2Cl_2 dropwise. Upon completion (by TLC), the reaction was quenched by adding cold MeOH. Solvent was removed under reduced pressure, and the residue was purified by column chromatography ($\text{MeOH}-\text{NH}_3$ (7 N), 2–10% in CH_2Cl_2) to afford 20 mg (75%) of 16c. ^1H NMR (500 MHz, CDCl_3) δ 7.84 (s, 1H), 7.80 (d, $J = 7.5$ Hz, 2H), 7.38–7.60 (m, 5H), 7.24 (m, 1H), 7.20 (t, $J = 8.0$ Hz, 1H), 6.88 (d, $J = 7.9$ Hz, 1H), 6.19 (d, $J = 8.4$ Hz, 1H), 3.88 (s, 3H), 3.65 (m, 4H), 2.61 (m, 4H), 2.41 (s, 3H). ^{13}C NMR (125 MHz, CDCl_3) δ 165.7, 162.8, 158.4, 147.7, 139.7, 138.5, 135.0, 131.8, 128.7, 129.4, 127.0, 122.8, 118.0, 117.2, 99.4, 99.1, 54.4, 53.7, 45.7, 44.4. HRMS (m/z): $[\text{M} + \text{H}]^+$ calcd for $\text{C}_{24}\text{H}_{27}\text{N}_4\text{O}_2\text{S}$, 435.1855; found, 435.1849.

2-Amino-*N*-(3-((2-methoxy-6-(4-methylpiperazin-1-yl)pyridin-3-yl)thio)phenyl)acetamide (16d). To a solution of 15 (20 mg, 0.06 mmol) in CH_2Cl_2 (1 mL) were added Boc-glycine (10.6 mg, 0.06 mmol), DMAP (1.0 mg), Et_3N (10 μL), and EDCI (11 mg, 0.06 mmol). The resulting solution was stirred at rt for 2 h. Solvent was evaporated under reduced pressure, and the residue was purified by column chromatography ($\text{CH}_2\text{Cl}_2/\text{MeOH}-\text{NH}_3$ (7 N), 1:0 to 85:15) to afford 26 mg (90%) of residue. To this was added 5 mL of 10% TFA- CH_2Cl_2 , and the resulting solution was stirred at rt for 1 h. Solvent was evaporated under reduced pressure, and the residue was purified by column chromatography ($\text{CH}_2\text{Cl}_2/\text{MeOH}-\text{NH}_3$ (7 N), 1:0 to 85:15) to afford 16 mg (85%) of 16d. ^1H NMR (500 MHz, CDCl_3): δ 9.26 (br s, 1H), 7.55 (d, $J = 8.0$ Hz, 1H), 7.47 (d, $J = 8.0$ Hz, 1H), 7.28 (s, 1H), 7.15 (t, $J = 8.0$ Hz, 1H), 6.82 (d, $J = 8.0$ Hz, 1H), 6.21 (d, $J = 8.0$ Hz, 1H), 3.89 (s, 3H), 3.62 (m, 4H), 3.42 (s, 2H), 2.54 (m, 4H), 2.36 (s, 3H). ^{13}C NMR (125 MHz, CDCl_3): δ 170.6, 162.7, 158.4, 147.5, 139.4, 138.0, 129.3, 122.5, 117.5, 116.5, 99.4, 98.9, 54.6, 53.6, 46.0, 45.1, 44.7. HRMS (m/z): $[\text{M} + \text{H}]^+$ calcd for $\text{C}_{19}\text{H}_{26}\text{N}_5\text{O}_2\text{S}$, 388.1807; found, 388.1808.

6-(4-Methylpiperazin-1-yl)pyridin-2-ol (17). A mixture of 11 (8.0 g, 0.0386 mol) in 50 mL of 48% HBr(aq) and a catalytic amount of tetrabutylammonium bromide was refluxed overnight. The reaction mixture was concentrated under reduced pressure and purified by column chromatography to give 5.1 g (68%) of 17. ^1H NMR (500 MHz, CDCl_3): δ 7.28–7.33 (m, 1H), 5.94 (d, $J = 8.7$ Hz, 1H), 5.54 (d, $J = 7.8$ Hz, 1H), 3.38 (m, 4H), 2.55 (m, 4H), 2.34 (s, 3H). ^{13}C NMR (125 MHz, CDCl_3): δ 165.2, 153.6, 142.6, 106.7, 90.6, 54.4, 47.3, 46.0. MS (m/z): $[\text{M} + \text{H}]^+$ 194.0.

1-(6-((4-Methoxybenzyl)oxy)pyridin-2-yl)-4-methylpiperazine (18). To a solution of 17 (1.2 g, 6.22 mmol) in DMF (40 mL) was added NaH (0.596 g, 24.8 mmol) at rt, and the mixture was stirred for 10 min. Then (PMB)Cl (1.06 g, 6.83 mmol) was added dropwise, and the mixture was stirred at rt for 1 h. The reaction mixture was concentrated under reduced pressure and purified by column chromatography to give 1.63 g (84%) of 18. MS (m/z): $[\text{M} + \text{H}]^+$ 314.2.

1-(5-Iodo-6-((4-methoxybenzyl)oxy)pyridin-2-yl)-4-methylpiperazine (19). To a solution of 18 (1.16 g, 3.7 mmol) in acetonitrile (50 mL) were added NIS (1.66 g, 7.4 mmol) and TFA (1.42 mL, 18.5 mmol), and the solution was stirred for 1 h at rt. The reaction mixture was concentrated under reduced pressure and purified by column chromatography to give 1.22 g (75%) of 19. MS (m/z): $[\text{M} + \text{H}]^+$ 440.0.

3-((2-((4-Methoxybenzyl)oxy)-6-(4-methylpiperazin-1-yl)pyridin-3-yl)thio)aniline (20). A mixture of 19 (452 mg, 1.03 mmol), 3-aminothiophenol (137 mg, 1.10 mmol), K_2CO_3 (552 mg, 4.0 mmol), neocuproine (45 mg, 0.2 mmol), and CuI (39 mg, 0.2 mmol) in DMF (10 mL) was heated to 130 $^\circ\text{C}$ for 16 h. Solvent was removed under reduced pressure, and the residue was purified by column

chromatography ($\text{CH}_2\text{Cl}_2/\text{MeOH}-\text{NH}_3$ (7 N), 1:0 to 85:15) to afford 224 mg (50%) of 20. MS (m/z): $[\text{M} + \text{H}]^+$ 437.2.

2-Amino-*N*-(3-((2-hydroxy-6-(4-methylpiperazin-1-yl)pyridin-3-yl)thio)phenyl)acetamide (21). To a solution of 20 (220 mg, 0.5 mmol) in CH_2Cl_2 (10 mL) were added Boc-glycine (96 mg, 0.55 mmol), DMAP (6.1 mg, 0.05 mmol), and EDCI (105 mg, 0.55 mmol). The resulting solution was stirred at rt for 2 h. Solvent was evaporated under reduced pressure, and the residue was purified by column chromatography ($\text{CH}_2\text{Cl}_2/\text{MeOH}-\text{NH}_3$ (7 N), 1:0 to 85:15) to afford a residue. To this was added 10 mL of 30% TFA/ CH_2Cl_2 , and the resulting solution was stirred at rt for 2 h. Solvent was evaporated under reduced pressure, and the residue was purified by column chromatography ($\text{CH}_2\text{Cl}_2/\text{MeOH}-\text{NH}_3$ (7N), 1:0 to 85:15) to afford 153 mg (82%) of 21. ^1H NMR (500 MHz, CDCl_3): δ 9.31 (br s, 1H), 7.62 (d, $J = 8.4$ Hz, 1H), 7.44 (d, $J = 8.0$ Hz, 1H), 7.31 (s, 1H), 7.19 (t, $J = 8.0$ Hz, 1H), 6.93 (d, $J = 7.8$ Hz, 1H), 5.58 (d, $J = 8.4$ Hz, 1H), 3.34 (s, 2H), 3.33 (m, 4H), 2.29 (m, 4H), 2.22 (s, 3H). HRMS (m/z): $[\text{M} + \text{H}]^+$ calcd for $\text{C}_{18}\text{H}_{24}\text{N}_5\text{O}_2\text{S}$, 374.1651; found, 374.1646.

4-(Benzyloxy)-2-chloropyrimidine (23a). To a solution of 2,4-dichloropyrimidine (22) (2.0 g, 0.0134 mmol) in toluene (20 mL) were added benzyl alcohol (1.53 mL, 1.59 g, 0.0147 mol), KOH (0.82 g, 0.0147 mol), and 18-crown-6 (0.177 g, 0.00067 mol), and the resulting solution was stirred at rt for 1 h. The reaction mixture was diluted with EtOAc (400 mL), washed with water (3 \times 50 mL), dried over MgSO_4 , filtered, and concentrated to give a white solid that was chromatographed (hexane/ CH_2Cl_2 , 1:1 to 3:7) to afford 2.09 g (71%) of a mixture of 23a with regioisomeric 2-(benzyloxy)-4-chloropyrimidine (relative ratio 75:25 by ^1H NMR, respectively). MS (m/z): $[\text{M} + \text{Na}]^+$ 243.1.

4-(Benzyloxy)-2-(4-methylpiperazin-1-yl)pyrimidine (24a). To a solution of 23a (2.09 g, 0.00947 mol; contains regioisomer) in DMF (34 mL) was added 1-methylpiperazine (3.15 mL, 2.85 g, 0.0284 mol), and the resulting solution was heated at 80 $^\circ\text{C}$ for 1.75 h. Solvent was removed under reduced pressure, and the residue was taken up into EtOAc (350 mL) and washed with brine (3 \times 50 mL). The aqueous layer was extracted with EtOAc (2 \times 50 mL), and the combined organic layers were dried over MgSO_4 , filtered, and concentrated to give an oil that was purified by column chromatography (EtOAc/ $\text{MeOH}-\text{NH}_3$ (7 N), 1:0 to 25:1) to afford 1.88 g (70%) of 24a. ^1H NMR (500 MHz, CDCl_3): δ 8.06 (d, $J = 5.6$ Hz, 1H), 7.41 (d, $J = 7.0$ Hz, 2H), 7.35 (t, $J = 7.0$ Hz, 2H), 7.32 (d, $J = 7.0$ Hz, 1H), 6.03 (d, $J = 5.6$ Hz, 1H), 5.35 (s, 2H), 3.83 (m, 4H), 2.45 (m, 4H), 2.33 (s, 3H). MS (m/z): $[\text{M} + \text{H}]^+$ 284.9.

4-(Benzyloxy)-5-iodo-2-(4-methylpiperazin-1-yl)pyrimidine (25a). To 24a (0.937 g, 0.0033 mol) in acetonitrile (16 mL) were added TFA (1.02 mL, 1.51 g, 0.0132 mol) and *N*-iodosuccinimide (0.965 g, 0.0043 mol), and the resulting solution was stirred at rt for 1 h. Then 7 mL of 10% Na_2CO_3 (0.70 g, 0.066 mol) was added, and the resulting solution was stirred for 2 min. The reaction mixture was concentrated to dryness, and the residue was taken up into CH_2Cl_2 (200 mL) and washed with 10% Na_2CO_3 (2 \times 50 mL), 10% sodium thiosulfate (50 mL), and brine (50 mL). The organic layer was dried over MgSO_4 , filtered, and concentrated to give an oil which was purified by column chromatography ($\text{CH}_2\text{Cl}_2/\text{MeOH}-\text{NH}_3$ (7 N), 50:1) to yield 1.31 g (97%) of 25a. ^1H NMR (500 MHz, CDCl_3): δ 8.27 (s, 1H), 7.44 (d, $J = 7.4$ Hz, 2H), 7.37 (t, $J = 7.2$ Hz, 2H), 7.32 (d, $J = 7.3$ Hz, 1H), 5.40 (s, 2H), 3.79 (m, 4H), 2.42 (m, 4H), 2.32 (s, 3H). MS (m/z): $[\text{M} + \text{H}]^+$ 411.0.

3-((4-(Benzyloxy)-2-(4-methylpiperazin-1-yl)pyrimidin-5-yl)thio)aniline (26a). A mixture of 25a (0.985 g, 2.40 mmol), 3-aminobenzenethiol (255 μL , 300.5 mg, 2.40 mmol), neocuproine (150 mg, 0.72 mmol), copper iodide (137 mg, 0.72 mmol), and potassium carbonate (0.663 g, 4.80 mmol) in DMF (25 mL) was stirred at 120 $^\circ\text{C}$ for 18 h. Solvent was removed under reduced pressure, and the residue was purified by column chromatography ($\text{CH}_2\text{Cl}_2/\text{MeOH}-\text{NH}_3$ (7 N), 50:1 to 20:1) to afford 0.75 g (77%) of 26a. ^1H NMR (500 MHz, CDCl_3): δ 8.24 (s, 1H), 7.16–7.30 (m, 5H), 6.99 (t, $J = 7.3$ Hz, 1H), 6.56 (d, $J = 7.6$ Hz, 1H), 6.38–6.46 (m, 2H), 5.38 (s, 2H), 3.84 (m, 4H), 3.56 (br s, 2H), 2.45 (br s, 4H), 2.33 (s, 3H). ^{13}C NMR (125 MHz, CDCl_3): δ 169.3, 164.5, 161.4, 158.1,

146.9, 138.5, 136.8, 129.6, 128.3, 127.7, 127.4, 117.6, 113.6, 112.6, 67.6, 54.8, 46.2, 43.9. MS (*m/z*): [M + H]⁺ 408.1.

N-(3-((4-(Benzyloxy)-2-(4-methylpiperazin-1-yl)pyrimidin-5-yl)thio)phenyl)acetamide (**27a**). To **26a** (5.2 mg, 0.013 mmol) in CH₂Cl₂ (0.2 mL) was added acetic anhydride (1.5 μL, 1.6 mg, 0.0156 mmol), and the resulting solution was stirred at rt for 4 h. The solution was then concentrated to dryness under reduced pressure to give a residue which was purified by preparatory TLC (CH₂Cl₂/MeOH–NH₃ (7 N), 20:1) to afford 4.5 mg (79%) of **27a**. ¹H NMR (500 MHz, CDCl₃/MeOH-*d*₄): δ 8.24 (s, 1H), 7.54 (d, *J* = 7.7 Hz, 1H), 7.22–7.27 (m, 3H), 7.13–7.20 (m, 3H), 7.09 (s, 1H), 6.87 (d, *J* = 7.7 Hz, 1H), 5.36 (s, 2H), 3.85 (m, 4H), 2.49 (m, 4H), 2.35 (s, 3H), 2.10 (s, 3H). MS (*m/z*): [M + H]⁺ 450.1.

N-(3-((4-(Benzyloxy)-2-(4-methylpiperazin-1-yl)pyrimidin-5-yl)thio)phenyl)benzamide (**27b**). **26a** (14 mg, 0.034 mmol), Et₃N (24 μL, 17.2 mg, 0.17 mmol), and benzoyl chloride (12 μL, 14.3 mg, 0.102 mmol) in CH₂Cl₂ (1 mL) were stirred at rt for 2 h. Solvent was removed under reduced pressure, and the residue was purified by preparatory TLC (CH₂Cl₂/MeOH–NH₃ (7 N), 25:1) to afford 13.6 mg (78%) of **27b**. ¹H NMR (500 MHz, CDCl₃/MeOH-*d*₄): δ 8.26 (s, 1H), 7.84 (d, *J* = 7.4 Hz, 2H), 7.69 (dd, *J* = 1.4, 8.2 Hz, 1H), 7.54 (t, *J* = 7.3 Hz, 1H), 7.47 (t, *J* = 7.9 Hz, 2H), 7.14–7.27 (m, 7H), 6.93 (dd, *J* = 0.9, 7.9 Hz, 1H), 5.37 (s, 2H), 3.85 (m, 4H), 2.48 (m, 4H), 2.35 (s, 3H). ¹³C NMR (125 MHz, CDCl₃/MeOH-*d*₄): δ 168.6, 166.3, 164.2, 161.3, 138.6, 138.3, 136.4, 134.8, 131.8, 129.3, 128.6, 128.3, 127.7, 127.5, 127.2, 123.4, 118.8, 117.9, 100.1, 67.8, 54.6, 45.9, 43.6. MS (*m/z*): [M + H]⁺ 512.1.

2-Amino-*N*-(3-((4-(benzyloxy)-2-(4-methylpiperazin-1-yl)pyrimidin-5-yl)thio)phenyl)acetamide (**27c**). To **26a** (30 mg, 0.0736 mmol) in THF (3 mL) were added Boc-glycine (14.2 mg, 0.081 mmol) and DCC (16.7 mg, 0.081 mmol), and the resulting solution was stirred at rt overnight. The reaction mixture was concentrated under reduced pressure, the residue was purified by preparatory TLC (CH₂Cl₂/MeOH–NH₃ (7 N), 25:1) to afford an oil which was dissolved in 2.5 mL of CH₂Cl₂/TFA (4:1), and the resulting solution was stirred at rt for 45 min. The reaction mixture was concentrated under reduced pressure, and the residue was purified by preparatory TLC (CH₂Cl₂/MeOH–NH₃ (7 N), 15:1) to afford 24.6 mg (72%) of **27c**. ¹H NMR (500 MHz, CDCl₃/MeOH-*d*₄): δ 8.24 (s, 1H), 7.50 (dd, *J* = 1.2, 8.1 Hz, 1H), 7.31 (m, 1H), 7.22–7.27 (m, 3H), 7.13–7.20 (m, 3H), 6.86 (d, *J* = 7.9 Hz, 1H), 5.37 (s, 2H), 3.85 (m, 4H), 3.39 (s, 2H), 2.49 (m, 4H), 2.35 (s, 3H). ¹³C NMR (125 MHz, CDCl₃/MeOH-*d*₄): δ 171.4, 168.5, 164.1, 161.2, 138.2, 138.1, 136.4, 129.2, 128.2, 127.6, 127.2, 123.0, 118.2, 117.0, 67.7, 54.5, 45.8, 44.6, 43.5. MS (*m/z*): [M + H]⁺ 465.3.

2-Amino-*N*-(3-((4-(benzyloxy)-2-(4-methylpiperazin-1-yl)pyrimidin-5-yl)thio)phenyl)propanamide (**27d**). To **26a** (8.4 mg, 0.0206 mmol) in THF (0.5 mL) were added Boc-L-alanine (5.6 mg, 0.0227 mmol) and DCC (4.7 mg, 0.0227 mmol), and the resulting solution was stirred at rt overnight. The reaction mixture was concentrated under reduced pressure, the residue was dissolved in 0.35 mL of CH₂Cl₂/TFA (4:1), and the resulting solution was stirred at rt for 45 min. The reaction mixture was concentrated under reduced pressure, and the residue was purified by preparatory TLC (CH₂Cl₂/MeOH–NH₃ (7 N), 15:1) to afford 4.1 mg (41%) of **27d**. ¹H NMR (500 MHz, CDCl₃): δ 9.34 (s, 1H), 8.26 (s, 1H), 7.59 (d, *J* = 8.2 Hz, 1H), 7.20–7.30 (m, 4H), 7.12–7.19 (m, 3H), 6.85 (m, 1H), 5.37 (s, 2H), 3.81–3.91 (m, 4H), 3.60 (q, *J* = 7.0 Hz, 1H), 2.43–2.52 (m, 4H), 2.35 (s, 3H), 1.42 (d, *J* = 7.0 Hz, 3H). MS (*m/z*): [M + H]⁺ 479.4.

2-Amino-*N*-(3-((4-(benzyloxy)-2-(4-methylpiperazin-1-yl)pyrimidin-5-yl)thio)phenyl)-3-methylbutanamide (**27e**). To **26a** (6.6 mg, 0.0162 mmol) in THF (0.5 mL) were added Boc-L-valine (4.1 mg, 0.0178 mmol) and DCC (3.7 mg, 0.0178 mmol), and the resulting solution was stirred at rt overnight. The reaction mixture was concentrated under reduced pressure, the residue was dissolved in 0.35 mL of CH₂Cl₂/TFA (4:1), and the resulting solution was stirred at rt for 45 min. The reaction mixture was concentrated under reduced pressure, and the residue was purified by preparatory TLC (CH₂Cl₂/MeOH–NH₃ (7 N), 15:1) to afford 4.4 mg (54%) of **27e**. ¹H NMR

(500 MHz, CDCl₃): δ 9.39 (s, 1H), 8.26 (s, 1H), 7.60 (d, *J* = 8.0 Hz, 1H), 7.20–7.34 (m, 4H), 7.12–7.19 (m, 3H), 6.84 (d, *J* = 7.8 Hz, 1H), 5.37 (s, 2H), 3.81–3.92 (m, 4H), 3.36 (m, 1H), 2.39–2.52 (m, 5H), 2.35 (s, 3H), 1.04 (d, *J* = 6.8 Hz, 3H), 0.86 (d, *J* = 6.7 Hz, 3H). MS (*m/z*): [M + H]⁺ 507.2.

N-(3-((4-(Benzyloxy)-2-(4-methylpiperazin-1-yl)pyrimidin-5-yl)thio)phenyl)pyrrolidine-2-carboxamide (**27f**). To **26a** (8.6 mg, 0.0211 mmol) in THF (0.5 mL) were added Boc-L-proline (5 mg, 0.0232 mmol) and DCC (5 mg, 0.0232 mmol), and the resulting solution was stirred at rt overnight. The reaction mixture was concentrated under reduced pressure, the residue was dissolved in 0.35 mL of CH₂Cl₂/TFA (4:1), and the resulting solution was stirred at rt for 45 min. The reaction mixture was concentrated under reduced pressure, and the residue was purified by preparatory TLC (CH₂Cl₂/MeOH–NH₃ (7 N), 15:1) to afford 6.0 mg (57%) of **27f**. ¹H NMR (500 MHz, CDCl₃): δ 9.63 (s, 1H), 8.26 (s, 1H), 7.58 (dd, *J* = 1.2, 8.1 Hz, 1H), 7.31 (t, *J* = 1.9 Hz, 1H), 7.12–7.17 (m, 3H), 7.22–7.26 (m, 3H), 6.83 (d, *J* = 7.9 Hz, 1H), 5.36 (s, 2H), 3.80–3.91 (m, 5H), 3.04–3.11 (m, 1H), 2.94–3.00 (m, 1H), 2.47 (m, 4H), 2.35 (s, 3H), 2.15–2.25 (m, 1H), 1.98–2.06 (m, 1H), 1.70–1.81 (m, 1H). MS (*m/z*): [M + H]⁺ 505.2.

2-Chloro-4-phenylpyrimidine (**23b**). To a mixture of **22** (50 mg, 0.336 mmol), phenylboronic acid (41 mg, 0.336 mmol), sodium carbonate (110 mg in 0.5 mL of water), and DME (2.5 mL) were added palladium acetate (3.8 mg, 0.0168 mmol) and triphenylphosphine (8.8 mg, 0.0336 mmol). The reaction mixture was heated at 95 °C for 20 h. Solvent was removed under reduced pressure and the residue taken up into dichloromethane (20 mL), washed with water (3 × 5 mL), dried over MgSO₄, and concentrated to give a residue which was purified by preparatory TLC (hexane/EtOAc, 8:2) to yield 41 mg (64%) of **23b**. ¹H NMR (500 MHz, CDCl₃): δ 8.63 (d, *J* = 5.2 Hz, 1H), 8.06–8.11 (m, 2H), 7.64 (d, *J* = 5.3 Hz, 1H), 7.47–7.57 (m, 3H). ¹³C NMR (125 MHz, CDCl₃): δ 167.2, 161.9, 159.8, 135.1, 131.9, 129.1, 127.4, 115.2.

2-(4-Methylpiperazin-1-yl)-4-phenylpyrimidine (**24b**). To a solution of **23b** (38 mg, 0.201 mmol) in 0.5 mL of DMF was added 1-methylpiperazine (56 μL, 50 mg, 0.31 mmol), and the resulting solution was heated at 90 °C for 1.5 h. Solvent was removed under reduced pressure, and the residue was purified by preparatory TLC (CH₂Cl₂/MeOH–NH₃ (7 N), 20:1) to yield 49 mg (95%) of **24b**. ¹H NMR (500 MHz, CDCl₃): δ 8.36 (d, *J* = 5.2 Hz, 1H), 8.01–8.09 (m, 2H), 7.43–7.50 (m, 3H), 6.92 (d, *J* = 5.2 Hz, 1H), 3.96 (m, 4H), 2.50 (m, 4H), 2.34 (s, 3H). ¹³C NMR (125 MHz, CDCl₃): δ 164.4, 162.1, 158.4, 137.8, 130.6, 128.8, 127.1, 105.8, 55.2, 46.4, 43.9. MS (*m/z*): [M + H]⁺ 255.1.

5-Iodo-2-(4-methylpiperazin-1-yl)-4-phenylpyrimidine (**25b**). To **24b** (49 mg, 0.193 mmol) in acetonitrile (1.4 mL) were added TFA (59 μL, 88 mg, 0.772 mmol) and *N*-iodosuccinimide (43 mg, 0.193 mmol), and the resulting solution was stirred at rt for 1 h. Solvent was evaporated, and the residue was taken up into dichloromethane (15 mL), washed with 10% Na₂CO₃ (2 × 5 mL) and water (5 mL), dried over MgSO₄, and concentrated to give a residue which was purified by preparatory TLC (CH₂Cl₂/MeOH, 10:1) to yield 67 mg (92%) of **25b**. ¹H NMR (500 MHz, CDCl₃): δ 8.60 (s, 1H), 7.65–7.73 (m, 2H), 7.42–7.49 (m, 3H), 3.86 (m, 4H), 2.45 (m, 4H), 2.33 (s, 3H). ¹³C NMR (125 MHz, CDCl₃): δ 167.5, 165.8, 160.9, 140.3, 129.7, 129.3, 128.1, 76.2, 55.0, 46.4, 43.9. MS (*m/z*): [M + H]⁺ 380.9.

3-((2-(4-Methylpiperazin-1-yl)-4-phenylpyrimidin-5-yl)thio)aniline (**26b**). A mixture of **25b** (37.6 mg, 0.099 mmol), 3-aminobenzenethiol (12 μL, 13.6 mg, 0.109 mmol), neocuproine (6.2 mg, 0.0297 mmol), copper iodide (5.7 mg, 0.0297 mmol), and potassium carbonate (42 mg, 0.198 mmol) in DMF (1.4 mL) was stirred at 110 °C for 12 h. Solvent was removed under reduced pressure, and the residue was purified by preparatory TLC (CH₂Cl₂/MeOH–NH₃ (7 N), 10:1) to afford 10 mg (27%) of **26b**. ¹H NMR (500 MHz, CDCl₃): δ 8.45 (s, 1H), 7.71 (d, *J* = 6.6 Hz, 2H), 7.32–7.42 (m, 3H), 6.99 (t, *J* = 7.9 Hz, 1H), 6.47 (d, *J* = 7.8 Hz, 1H), 6.43 (dd, *J* = 2.0, 6.4 Hz, 1H), 6.36 (d, *J* = 1.8 Hz, 1H), 3.97 (m, 4H), 3.60 (br s, 2H), 2.52 (m, 4H), 2.37 (s, 3H). MS (*m/z*): [M + H]⁺ 378.1.

2-Amino-N-(3-((2-(4-methylpiperazin-1-yl)-4-phenylpyrimidin-5-yl)thio)phenyl)acetamide (27g). To a solution of **26b** (5 mg, 0.0133 mmol) in THF (0.5 mL) were added Boc-glycine (2.3 mg, 0.0133 mmol) and DCC (3 mg, 0.0146 mmol). After the resulting solution was stirred for 2 h at rt, THF was evaporated, and 0.5 mL of CH₂Cl₂/TFA (4:1) was added. The solution was stirred for 45 min and then concentrated to dryness under reduced pressure to give a residue which was purified by preparatory TLC (CH₂Cl₂/MeOH–NH₃ (7 N), 10:1) to afford 2 mg (35%) of **27g**. ¹H NMR (500 MHz, CDCl₃/MeOH-*d*₄): δ 8.45 (s, 1H), 7.69 (d, *J* = 8.2 Hz, 2H), 7.35–7.45 (m, 4H), 7.31 (m, 1H), 7.17 (t, *J* = 8.0 Hz, 1H), 6.76 (d, *J* = 7.8 Hz, 1H), 3.96 (m, 4H), 3.36 (s, 2H), 2.56 (m, 4H), 2.38 (s, 3H). MS (*m/z*): [M + H]⁺ 435.0.

Biological Testing. Cell Lines. SKBr3 cells were a gift from Dr. Neal Rosen (Memorial Sloan-Kettering Cancer Center, MSKCC) and Kasumi-1 and MOLM-13 from Dr. Stephen Nimer (MSKCC). MDA-MB-468 and Mia-PaCa-2 cell lines were purchased from ATCC. Cells were cultured routinely in DME/F12 (SKBr3, MDA-MB-468, Mia-PaCa-2) or in RPMI (Kasumi-1, MOML-13) supplemented with 10% fetal bovine serum, 1% L-glutamine, 1% penicillin, and streptomycin.

Western Blotting. Cells were grown to 60–70% confluence and treated with inhibitor or DMSO vehicle for the indicated times. Protein lysates were prepared in 50 mM Tris, pH 7.4, 150 mM NaCl, and 1% NP-40 lysis buffer. Protein concentrations were measured using the BCA kit (Pierce) according to the manufacturer's instructions. Protein lysates (10–50 μg) were resolved by SDS-PAGE, transferred onto a nitrocellulose membrane, and incubated with the indicated primary antibodies: anti-HER2 from rabbit (1:250, 28-0004, Zymed), anti-Raf-1 from rabbit (1:500, sc-133, Santa Cruz), anti-PARP (p85 fragment) from rabbit (1:500, G7341, Promega), anti-β-actin from mouse (1:2500, A1978, Sigma-Aldrich), anti-Akt from rabbit (1:500, 9272, Cell Signaling), anti-p-STAT3 (Y705) from rabbit (1:500, 9145, Cell Signaling), anti-p-STAT5 (Y694) from rabbit (1:500, 9351, Cell Signaling), anti-FLT3 from rabbit (1:500, sc-480, Santa Cruz), anti-HOP from mouse (1:500, SRA-1500, Enzo), and anti-Hsp/c70 from mouse (1:2000, smc-106B, Stressmarq). Membranes were then incubated with a corresponding peroxidase-conjugated secondary antibody (1:3000 dilution).

Hsp90 Binding Assay. For the competition studies, fluorescence polarization (FP) assays were performed as previously reported.³⁶ Briefly, FP measurements were performed on an Analyst GT instrument (Molecular Devices, Sunnyvale, CA). Measurements were taken in black 96-well microtiter plates (Corning no. 3650) where both the excitation and the emission occurred from the top of the wells. A stock of 10 μM GM-cy3B was prepared in DMSO and diluted with Felts buffer (20 mM HEPES (K), pH 7.3, 50 mM KCl, 2 mM DTT, 5 mM MgCl₂, 20 mM Na₂MoO₄, and 0.01% NP40 with 0.1 mg/mL BGG). To each 96-well plate were added 6 nM fluorescent GM (GM-cy3B), 3 μg of SKBr3 lysate (total protein), and tested inhibitor (initial stock in DMSO) in a final volume of 100 μL of HFB buffer. Drugs were added in triplicate wells. For each assay, background wells (buffer only), tracer controls (free, fluorescent GM only), and bound GM controls (fluorescent GM in the presence of SKBr3 lysate) were included on each assay plate. GM was used as a positive control. The assay plate was incubated on a shaker at 4 °C for 24 h, and the FP values (mP) were measured. The fraction of tracer bound to Hsp90 was correlated to the FP value and plotted against the values of competitor concentrations. The inhibitor concentration at which 50% of bound GM was displaced was obtained by fitting the data. All experimental data were analyzed using SOFTmax Pro 4.3.1 and plotted using Prism 4.0 (Graphpad Software Inc., San Diego, CA).

Growth Inhibition Assay. We evaluated the antiproliferative effects of inhibitors using the dye Alamar Blue. This reagent offers a rapid objective measure of cell viability in cell culture, and it uses the indicator dye resazurin to measure the metabolic capacity of cells, an indicator of cell viability. Briefly, cells were plated on Costar 96-well plates. For attached cells (such as SKBr3), 8000 cells/well were used. For suspension cells (such as Kasumi-1), 20000 cells/well were plated. Cells were allowed to incubate for 24 h at 37 °C before drug treatment. Drugs were added in triplicate at the indicated

concentrations, and the plate was incubated for 72 h. Alamar Blue (50 μM) was added and the plate read 6 h later using the Analyst GT (fluorescence intensity mode, excitation 530 nm, emission 580 nm, with a 560 nm dichroic mirror). Results were analyzed using the Softmax Pro software. The percentage cell growth inhibition was calculated by comparing fluorescence readings obtained from treated versus control cells, accounting for the initial cell population (time zero). IC₅₀ was calculated as the drug concentration that inhibits cell growth by 50%.

Caspase-3,7 Activation.³⁷ MOLM-13 cells (30000 cells/well) were plated in black 96-well plates (Corning no. 3603) in 40 μL of RPMI medium and left in an incubator (37 °C, 5% CO₂) for up to 24 h. Cells were treated for 16 h with compounds or DMSO (control) at the desired concentrations in 50 μL of medium. Following exposure of cells to Hsp70 inhibitors, 50 μL of buffer containing 10 mM HEPES (pH 7.5), 2 mM EDTA, 0.1% CHAPS, and the caspase substrate Z-DEVD-R110 at 25 μM was added to each well. Plates were incubated until the signal stabilized, and then the fluorescence signal of each well was measured in an Analyst GT microplate reader. The percentage increase in apoptotic cells was calculated by comparison of the fluorescence reading obtained from treated versus control cells.

Hsp70–HOP Complex Analysis. SKBr3 cells were treated with the indicated concentrations of the inhibitor for 24 h. Samples were collected and lysed in 20 mM Tris, pH 7.4, 25 mM NaCl, 0.1% NP-40 buffer with protease inhibitors added. Aliquots of 500 μg of total protein adjusted to 100 μL with the lysis buffer were prepared. Samples were incubated with 5 μL of BB70 antibody (Stressmarq) or normal IgG (as a negative control) and 20 μL of protein G agarose beads (Upstate) at 4 °C overnight. Samples were washed five times with the lysis buffer and applied to SDS-PAGE followed by a standard Western blotting procedure to detect levels of HOP protein in the Hsp/c70 complexes upon treatment.

Hsp70 Luciferase Refolding in Cells. The refolding of heat-denatured luciferase was assayed as described.³⁵ HEK293 cells were transfected with 2 μg of luciferase plasmid and 8 μg of Hsp70 plasmid or control vector per 60 mm dish. Human Hsp70, Hsp70-C267S, and Hsc70 were N-terminally Flag-tagged, and luciferase was C-terminally HA-tagged in pcDNA3.1. Two days after transfection, cells were treated with cycloheximide (Sigma) at 50 μg/mL to inhibit protein synthesis, transferred to 45 °C for 1 h, and then brought back to 37 °C for up to 2 h of recovery. **27c** was added immediately before heat shock. Cell samples, taken before heat shock and at 0, 1, and 2 h of recovery, were lysed on ice with PBS containing 1% Triton X-100, and the insoluble material was removed by centrifugation at 20000g. Total protein amounts in the supernatants were determined using the BCA Protein Assay Kit (Pierce). Luciferase enzymatic activities in the supernatants were measured using the Luciferase Reporter Assay Kit (Promega) and activity values normalized to total protein amounts.

Cycloheximide Treatments. Cells were treated with cycloheximide (at a final concentration of 100 μg/mL) with added vehicle (DMSO) or **27c** (20 μM) for the indicated times. Cells were lysed as indicated above, and the resulting samples were analyzed by Western blotting.

■ ASSOCIATED CONTENT

Accession Codes

The PDB ID codes of crystal structures used as a starting point for building the homology model are 1S3X, 2KHO, and 2P32.

■ AUTHOR INFORMATION

Corresponding Authors

*Phone: 646-888-2238. E-mail: taldonet@mskcc.org.

*Phone: 646-888-2235. E-mail: chiosisg@mskcc.org.

Present Addresses

[§]Y.K.: BioZone Pharmaceuticals Inc., 710 Fox Run Dr., Plainsboro, NJ 08536.

^{||}A.G.: Albany Medical Center, 43 New Scotland Ave., Albany, NY 12208.

[†]C.C.C.: Albert Einstein College of Medicine, 1300 Morris Park Ave., Bronx, NY 10461.

Notes

The authors declare no competing financial interest.

ACKNOWLEDGMENTS

We are supported in part by MSKCC's Technology Transfer Fund (G.C., A.R., Y.K.), Department of Defense Grant W81XWH-10-1-0490 (T.T.), Susan G. Komen for the Cure (T.T., G.C.), the SPORE Pilot Award and Research & Therapeutics Program in Prostate Cancer (G.C.), NIH Grant R01 CA119001 (G.C.), Clinical and Translational Science Center (CTSC) Grant UL1 RR024996 (A.G.), the Breast Cancer Research Fund (G.C.), the Leukemia and Lymphoma Society (G.C.), the Hirshberg Foundation for Pancreatic Cancer (G.C.), and NIH Grants 1U01 AG032969-01A1 (G.C.) and 1R01 CA155226-01 (G.C.). We thank Dr. George Sukenick and Dr. Hui Liu of the NMR Analytical Core Facility at MSKCC for expert mass spectral analysis and Matthew Dankner and Allison Mackay for technical assistance.

ABBREVIATIONS USED

Hsp70, heat shock protein 70; Hsp90, heat shock protein 90; HOP, heat shock organizing protein; HSF-1, heat shock factor 1; HIP, Hsp70-interacting protein; CyP40, cyclophilin 40; HER2, human epidermal growth factor receptor 2; IP, Immunoprecipitation; STAT3, signal transducer and activator of transcription 3; STAT5, signal transducer and activator of transcription 5; PARP, poly(ADP-ribose) polymerase; Hsp40, heat shock protein 40; Hsp110, heat shock protein 110

REFERENCES

- (1) Mayer, M. P.; Bukau, B. Hsp70 chaperones: cellular functions and molecular mechanism. *Cell. Mol. Life Sci.* **2005**, *62*, 670–684.
- (2) Bukau, B.; Weissman, J.; Horwich, A. Molecular chaperones and protein quality control. *Cell* **2006**, *125*, 443–451.
- (3) Powers, M. V.; Jones, K.; Barillari, C.; Westwood, I.; van Montfort, R. L.; Workman, P. Targeting HSP70: the second potentially druggable heat shock protein and molecular chaperone? *Cell Cycle* **2010**, *9*, 1542–1550.
- (4) Rerole, A.-L.; Jago, G.; Garrido, C. Hsp70: anti-apoptotic and tumorigenic protein. *Methods Mol. Biol.* **2011**, *787*, 205–229.
- (5) Brodsky, J. F.; Chiosis, G. Hsp70 molecular chaperones: emerging roles in human disease and identification of small molecule modulators. *Curr. Top. Med. Chem.* **2006**, *6*, 1215–1225.
- (6) Pratt, W. B.; Toft, D. O. Regulation of signaling protein function and trafficking by the hsp90/hsp70-based chaperone machinery. *Exp. Biol. Med. (Maywood, NJ, U. S. A.)* **2003**, *228*, 111–133.
- (7) Wegele, H.; Müller, L.; Buchner, J. Hsp70 and Hsp90—a relay team for protein folding. *Rev. Physiol. Biochem. Pharmacol.* **2004**, *151*, 1–44.
- (8) Taipale, M.; Jarosz, D. F.; Lindquist, S. HSP90 at the hub of protein homeostasis: emerging mechanistic insights. *Nat. Rev. Mol. Cell Biol.* **2010**, *11*, 515–528.
- (9) Trepel, J.; Mollapour, M.; Giaccone, G.; Neckers, L. Targeting the dynamic HSP90 complex in cancer. *Nat. Rev. Cancer* **2010**, *10*, 537–549.
- (10) Garrido, C.; Brunet, M.; Didelot, C.; Zermati, Y.; Schmitt, E.; Kroemer, G. Heat shock proteins 27 and 70: anti-apoptotic proteins with tumorigenic properties. *Cell Cycle* **2006**, *5*, 2592–2601.
- (11) Powers, M. V.; Clarke, P. A.; Workman, P. Dual targeting of HSC70 and HSP72 inhibits HSP90 function and induces tumor-specific apoptosis. *Cancer Cell* **2008**, *14*, 250–262.
- (12) Patury, S.; Miyata, Y.; Gestwicki, J. E. Pharmacological targeting of the Hsp70 chaperone. *Curr. Top. Med. Chem.* **2009**, *9*, 1337–1351.

- (13) Evans, C. G.; Chang, L.; Gestwicki, J. E. Heat shock protein 70 (hsp70) as an emerging drug target. *J. Med. Chem.* **2010**, *53*, 4585–4602.

- (14) Kang, Y.; Taldone, T.; Patel, H. J.; Patel, P. D.; Rodina, A.; Gozman, A.; Maharaj, R.; Clement, C. C.; Patel, M. R.; Brodsky, J. L.; Young, J. C.; Chiosis, G. Heat shock protein 70 inhibitors. 1. 2,5'-thiodipyrimidine and 5-(phenylthio)pyrimidine acrylamides as irreversible binders to an allosteric site on heat shock protein 70. *J. Med. Chem.* **2014**, DOI: 10.1021/jm401551n.

- (15) Rodina, A.; Patel, P. D.; Kang, Y.; Patel, Y.; Baaklini, I.; Wong, M. J. H.; Taldone, T.; Yan, P.; Yang, C.; Maharaj, R.; Gozman, A.; Patel, M. R.; Patel, H. J.; Chirico, W.; Erdjument-Bromage, H.; Talele, T. T.; Young, J. C.; Chiosis, G. Identification of an allosteric pocket on human Hsp70 reveals a mode of inhibition of this therapeutically important protein. *Chem. Biol.* **2013**, *20*, 1469–1480.

- (16) Zou, J.; Guo, Y.; Guettouche, T.; Smith, D. F.; Voellmy, R. Repression of heat shock transcription factor HSF1 activation by HSP90 (HSP90 complex) that forms a stress-sensitive complex with HSF1. *Cell* **1998**, *94*, 471–480.

- (17) Barf, T.; Kaptein, A. Irreversible protein kinase inhibitors: balancing the benefits and risks. *J. Med. Chem.* **2012**, *55*, 6243–6262.

- (18) Singh, J.; Petter, R. C.; Baillie, T. A.; Whitty, A. The resurgence of covalent drugs. *Nat. Rev. Drug Discovery* **2011**, *10*, 307–317.

- (19) Ma, J. C.; Dougherty, D. A. The cation- π interaction. *Chem. Rev.* **1997**, *97*, 1303–1324.

- (20) Gallivan, J. P.; Dougherty, D. A. Cation- π interactions in structural biology. *Proc. Natl. Acad. Sci. U. S. A.* **1999**, *96*, 9459–9464.

- (21) Crowley, P. B.; Golovin, A. Cation- π interactions in protein-protein interfaces. *Proteins* **2005**, *59*, 231–239.

- (22) Meyer, E. A.; Castellano, R. K.; Diederich, F. Interactions with aromatic rings in chemical and biological recognition. *Angew. Chem., Int. Ed.* **2003**, *42*, 1210–1250.

- (23) Salonen, L. M.; Ellermann, M.; Diederich, F. Aromatic rings in chemical and biological recognition: energetics and structures. *Angew. Chem., Int. Ed.* **2011**, *50*, 4808–4842.

- (24) Sörme, P.; Arnoux, P.; Kahl-Knutsson, B.; Leffler, H.; Rini, J. M.; Nilsson, U. J. Structural and thermodynamic studies on cation- π interactions in lectin-ligand complexes: high-affinity galectin-3 inhibitors through fine-tuning of an arginine-arene interaction. *J. Am. Chem. Soc.* **2005**, *127*, 1737–1743.

- (25) Mecozzi, S.; West, J. A. P.; Dougherty, D. A. Cation- π interactions in aromatics of biological and medicinal interest: electrostatic potential surfaces as a useful qualitative guide. *Proc. Natl. Acad. Sci. U. S. A.* **1996**, *93*, 10566–10571.

- (26) Morgan, R. S.; Tatsch, C. E.; Gushard, R. H.; McAdon, J.; Warne, P. K. Chains of alternating sulfur and pi-bonded atoms in eight small proteins. *Int. J. Pept. Protein Res.* **1978**, *11*, 209–217.

- (27) Furet, P.; Bold, G.; Meyer, T.; Roessel, J.; Guagnano, V. Aromatic interactions with phenylalanine 691 and cysteine 828: a concept for FMS-like tyrosine kinase-3 inhibition. application to the discovery of a new class of potential antileukemia agents. *J. Med. Chem.* **2006**, *49*, 4451–4454.

- (28) Tsou, H. R.; Mamuya, N.; Johnson, B. D.; Reich, M. F.; Gruber, B. C.; Ye, F.; Nilakantan, R.; Shen, R.; Discafani, C.; DeBlanc, R.; Davis, R.; Koehn, F. E.; Greenberger, L. M.; Wang, Y. F.; Wissner, A. 6-Substituted-4-(3-bromophenylamino)quinazolines as putative irreversible inhibitors of the epidermal growth factor receptor (EGFR) and human epidermal growth factor receptor (HER-2) tyrosine kinases with enhanced antitumor activity. *J. Med. Chem.* **2001**, *44*, 2719–2734.

- (29) Wissner, A.; Overbeek, E.; Reich, M. F.; Floyd, M. B.; Johnson, B. D.; Mamuya, N.; Rosfjord, E. C.; Discafani, C.; Davis, R.; Shi, X.; Rabindran, S. K.; Gruber, B. C.; Ye, F.; Hallett, W. A.; Nilakantan, R.; Shen, R.; Wang, Y. F.; Greenberger, L. M.; Tsou, H. R. Synthesis and structure-activity relationships of 6,7-disubstituted 4-anilinoquinoline-3-carbonitriles. The design of an orally active, irreversible inhibitor of the tyrosine kinase activity of the epidermal growth factor receptor (EGFR) and the human epidermal growth factor receptor-2 (HER-2). *J. Med. Chem.* **2003**, *46*, 49–63.

(30) Tsou, H. R.; Overbeek-Klumpers, E. G.; Hallett, W. A.; Reich, M. F.; Floyd, M. B.; Johnson, B. D.; Michalak, R. S.; Nilakantan, R.; Discafani, C.; Golas, J.; Rabindran, S. K.; Shen, R.; Shi, X.; Wang, Y. F.; Upeslakis, J.; Wissner, A. Optimization of 6,7-disubstituted-4-(arylamino)quinoline-3-carbonitriles as orally active, irreversible inhibitors of human epidermal growth factor receptor-2 kinase activity. *J. Med. Chem.* **2005**, *48*, 1107–1131.

(31) Carmi, C.; Galvani, E.; Vacondio, F.; Rivara, S.; Lodola, A.; Russo, S.; Aiello, S.; Bordini, F.; Costantino, G.; Cavazzoni, A.; Alfieri, R. R.; Ardizzoni, A.; Petronini, P. G.; Mor, M. Irreversible inhibition of epidermal growth factor receptor activity by 3-aminopropanamides. *J. Med. Chem.* **2012**, *55*, 2251–2264.

(32) Young, J. C.; Agashe, V. R.; Siegers, K.; Hartl, F. U. Pathways of chaperone-mediated protein folding in the cytosol. *Nat. Rev. Mol. Cell Biol.* **2004**, *5*, 781–791.

(33) Bhangoo, M. K.; Tzankov, S.; Fan, A. C.; Dejgaard, K.; Thomas, D. Y.; Young, J. C. Multiple 40-kDa heat shock protein chaperones function in Tom70-dependent mitochondrial import. *Mol. Biol. Cell* **2007**, *18*, 3414–3428.

(34) Tzankov, S.; Wong, M. J. H.; Shi, K.; Nassif, C.; Young, J. C. Functional divergence between co-chaperones of Hsc70. *J. Biol. Chem.* **2008**, *283*, 27100–27109.

(35) Baaklini, I.; Wong, M. J.; Hantouche, C.; Patel, Y.; Shrier, A.; Young, J. C. The DNAJA2 substrate release mechanism is essential for chaperone-mediated folding. *J. Biol. Chem.* **2012**, *287*, 41939–41954.

(36) Du, Y.; Moullick, K.; Rodina, A.; Aguirre, J.; Felts, S.; Dingleline, R.; Fu, H.; Chiosis, G. High-throughput screening fluorescence polarization assay for tumor-specific Hsp90. *J. Biomol. Screening* **2007**, *12*, 915–924.

(37) Rodina, A.; Vilenchik, M.; Moullick, K.; Aguirre, J.; Kim, J.; Chiang, A.; Litz, J.; Clement, C. C.; Kang, Y.; She, Y.; Wu, N.; Felts, S.; Wipf, P.; Massague, J.; Jiang, X.; Brodsky, J. L.; Krystal, G. W.; Chiosis, G. Selective compounds define Hsp90 as a major inhibitor of apoptosis in small-cell lung cancer. *Nat. Chem. Biol.* **2007**, *3*, 498–507.